Supplementary Materials for

Predicting and manipulating cardiac drug inactivation by the human gut bacterium *Eggerthella lenta*

Henry J. Haiser, David B. Gootenberg, Kelly Chatman, Gopal Sirasani, Emily P. Balskus, and Peter J. Turnbaugh*
correspondence to: pturnbaugh@fas.harvard.edu

This PDF file includes:

Materials and Methods

Bacterial strains and culturing conditions

Eggerthella lenta and fecal community cultures grown in Bacto™ Brain Heart Infusion broth (BD) supplemented with arginine or other compounds as indicated. All cultures were grown at 37 °C in an anaerobic chamber (Coy laboratory products) under 2-5% H_2, 20% CO_2, and balance N_2. Bacterial growth curves were obtained by growth in a BioTek PowerWave 340 microplate spectrophotometer; growth curves and calculations were generated by the Gen5 v1.11 software package. *E. lenta* DSM2243 was obtained from DSMZ and the finished genome is available in NCBI GenBank (*9*). FAA 1-3-56 and 1-1-60 were obtained from Dr. Emma Allen-Vercoe (University of Guelph); draft genomes were sequenced by the Human Microbiome Project and are available in NCBI GenBank and the HMP Data Analysis and Coordination Center (http://www.hmpdacc.org). Cardiac glycosides were suspended in DMSO and supplemented in cultures as indicated; digoxin (D6003) and digitoxin (D5878) were purchased from Sigma; digoxigenin was obtained from Santa Cruz Biotechnology (sc_214892A); and ouabain from Enzo Life Sciences (BML-CM109-0001).

Ex vivo incubations

All human subjects gave informed consent before participating in this study, which was approved by the Harvard Committee on the Use of Human Subjects in Research. Frozen fecal samples were diluted 1:10 (w/v) in pre-reduced PBS. Diluted samples were homogenized and large particulate matter was allowed to settle. An aliquot of the resultant supernatant was removed and used to inoculate cultures in BHI broth containing digoxin (10 μg/mL) or vehicle control.

Gnotobiotic experiments

All experiments involving mice were performed with protocols approved by the Harvard Medical School Animal Studies Committee. Germ-free adult male Swiss-Webster mice were maintained in plastic gnotobiotic isolators under a strict 12-hour light cycle and fed

an autoclaved LF/PP chow (LabDiet autoclavable diet 5021) or irradiated diets (0% or 20%; Harlan-Teklad diets 93328 and 91352) *ad libitum* (**table S8** details chow consumption and mouse weight throughout the experiments). Colonization was performed by a single gavage of ~10^8 colony-forming units of *E. lenta*. Mice were subsequently maintained in cages in a gnotobiotic isolator. A digoxin stock solution (2 mg/mL in 2.6 M 1,2-propanediol, 8.7 M ethanol, 0.1 M glucose) was diluted in 0.3 M glucose to 0.02 mg/mL for oral administration into the stomach using a blunt-ended needle .

Fecal, urine, and serum sample preparation and ELISA

Fecal samples (~100-300 mg) were weighed, homogenized in 700 µL methanol:acetonitrile (1:2), and centrifuged at 8,000 x g for 5 minutes. The supernatant containing the extracted drug was saved, and the extraction procedure was repeated on the pellet; this typically resulted in ~1 mL of pooled supernatant. A 50 µL aliquot of the pooled supernatant was then dried completely in a speed vacuum (45 °C; high vapor setting), and resuspended in 50 µL of normal human serum (Jackson ImmunoResearch) in order to standardize the analyte background for digoxin quantification. Digoxin was then quantified using the Accubind DIG ELISA (Monobind Inc.; Lake Forest, CA) following the manufacturers instructions. Cross-reactivity with dihydrodigoxin was determined to be 6.3% by dividing the concentration of digoxin giving 50% B/B_0 by the concentration of dihydrodigoxin giving 50% B/B_0, where B is the sample absorbance and B_0 represents the zero dose standard. Mouse serum and urine samples were diluted in normal human serum and loaded directly onto the Accubind DIG ELISA for quantification as with the fecal samples. To ensure that the samples were within the analytical range of the assay, serum was typically diluted 1/30 while urine was diluted 1/100.

RNA-Seq sample preparation

Methods for microbial mRNA sequencing and analysis were as previously described (*13*) (**fig. S4**). Briefly, cells were lysed by a bead beater (BioSpec Products), total RNA was extracted with phenol:chloroform:isoamyl alcohol (pH 4.5, 125:24:1, Ambion 9720),

RNA was purified using MEGAClear columns (Ambion), and rRNA was depleted via subtractive hybridization (MICROBExpress, Ambion). cDNA was synthesized using SuperScript II and random hexamers (Invitrogen), followed by second strand synthesis with RNAseH and *E. coli* DNA polymerase (New England Biolabs). Samples were prepared for sequencing with an Illumina GAII instrument after enzymatic fragmentation (NEBE6040L/M0348S).

RNA-Seq analysis

A summary of our analysis pipeline is shown in **fig. S4**. All trimmed reads were mapped with SSAHA2 (*14*) to all predicted coding and non-coding genes from the *E. lenta* DSM2243 genome(s) (SSAHA2 parameters: -best 1 -score 20 -solexa). Adaptor, rRNA, and tRNA sequences were removed prior to further analysis. The number of transcripts assigned to each gene was tallied and normalized to reads per kilobase per million mapped reads (RPKM). To account for genes that are not detected due to limited sequencing depth, a 'pseudocount' of 1 was added to all samples. Each gene's expression value was normalized by z-score, a Spearman rank correlation distance matrix was constructed, clustered with UPGMA, and displayed in dendrogram format (Matlab version 7.12.0). Sets of significantly enriched or depleted genes were identified using the volcanofunc, mattest, and mafdr commands in Matlab (cutoffs: fold-change>2, FDR<0.05, unless otherwise noted). We also implemented a rank products analysis using the "RankProd" module in Bioconductor (*15*). For each comparison, normalized gene counts were grouped into 2 classes: controls and experiments. The module was then run using 100 permutations and "rand=123". We then output all gene clusters with a FDR<0.05 (cutoff=0.05, method="pfp"). Transcriptional profiles were graphed across the entire genome by performing a separate SSAHA2 mapping analysis against the finished *E. lenta* DSM2243 genome. Reads mapping to multiple locations were excluded from downstream analysis, counts at each base were natural log-transformed, and plots were generated in Matlab version 7.12.0 using the area function.

qRT-PCR/qPCR analysis

Total community DNA and RNA was extracted from gut contents or fecal samples. Samples were kept at -80 °C until extraction. Community DNA was isolated with the PowerSoil bacterial DNA extraction kit (MoBio, Carlsbad CA). Total RNA was used for cDNA synthesis prior to amplification (see above). Primers for the *cgr* operon, transporters, and the *E. lenta* 16S rRNA gene were designed using Primer3 (*16*) and validated for specificity by testing against pure cultures of *E. lenta* and other isolates (**table S4**). qRT-PCR assays are run using ABsoluteTM QPCR SYBR® Green ROX Mix (Thermo Scientific) on a Mx3000P QPCR System instrument (Stratagene, La Jolla, CA). Fold-changes were calculated relative to the 16S rRNA transcript using the $2^{-\Delta\Delta}$Ct method.

Comparative genomics

Reciprocal BLASTP comparisons were performed between all predicted protein sequences from the *E. lenta* DSM2243, strain 1-1-60, and strain 1-3-56 genomes using default parameters. We then identified all reciprocal and non-reciprocal best blast hits with an e-value$<10^{-5}$, score>50, and %identity>50. Genes without any significant homology to the other 2 genomes were marked as unique. MUMmer version 3.23 (*17*) was used to align each pair of bacterial genomes and to construct similarity plots (nucmer and mummerplot programs with default parameters).

LC/MS analyses

Detection of digoxin, dihydrodigoxin, and digitoxin was achieved by LC/MS analysis performed on an Agilent (Agilent Technologies, Santa Clara, CA) 6120 single-quadrupole LC/MS system. Masses for the [M - H+]- ions monitored via electrospray ionization in the negative ion mode employing a selective ion mode (SIM) technique were digoxin (779.4), dihydrodigoxin (781.9), and digitoxin (763.4). Mass spectrometer parameter settings were: drying gas (12.0 Lpm), nebulizer pressure (45.0 psi), drying gas temp (300 °C), vaporizer temp (225 °C), and capillary voltage (4000v). An external standard curve mixture was analyzed at various concentrations 0.2 ng/µL – 25 ng/µL and utilized for quantitation. Liquid chromatography conditions with an Agilent Eclipse XDB-C18, 4.6 x 150 mm column were as follows: flow rate = 0.4 mLs/min; solvent A =

1 mM ammonium bicarbonate in 10% MeOH; solvent B = 1mM ammonium bicarbonate in 100% MeOH; gradient: 70-100% B in 10 min, 100% B for 1.5 min, 70% B for 3.5 min.

LC/MS/MS analyses

Detection of digoxin, dihydrodigoxin, and digitoxin was achieved by LC/MS/MS analysis performed on an Agilent (Agilent Technologies, Santa Clara, CA) 6460 triple-quadrupole LC/MS/MS system. The [M - H+]- / product ions monitored via electrospray ionization in the negative ion mode with multiple reaction monitoring (MRM) were digoxin (779.4/649.3), dihydrodigoxin (781.9/521.3), and digitoxin (763.4/503.3). Mass spectrometer parameter settings were gas temp (350 °C), gas flow (12 L/min), nebulizer (25 psi), sheath gas temp (375 °C), sheath gas flow (12 L/min), capillary voltage (4000v), and nozzle voltage (500v). An external standard curve mixture was analyzed at various concentrations 10 pg/µL – 1000 pg/µL and utilized for quantitation. Liquid chromatography conditions with an Agilent Eclipse XDB-C18, 4.6 x 150 mm column were as follows: flow rate = 0.4 mLs/min; solvent A = 1 mM ammonium bicarbonate in 10% MeOH; solvent B = 1 mM ammonium bicarbonate in 100% MeOH; gradient: 70-100% B in 10 min, 100% B for 1.5 min, 70% B for 3.5 min.

LC/MS/MS analysis of underivatized amino acids

We analyzed samples collected from the distal small intestine (ileum), which were prepared by resuspending gastrointestinal contents (100-300 mg) in 1 mL dH_2O and mixing with 4.5 mL $CHCl_2$:MeOH (2:1). Samples were then centrifuged at 1000 rpm for 5 min, after which the supernatant was removed and the $CHCl_2$/MeOH extraction was repeated. Samples were either concentrated using a speed vacuum centrifuge and resuspended in dH_20, or run on the LC/MS directly. LC/MS/MS analysis of amino acids was based on a previously described method (*18*), with an Agilent (Agilent Technologies, Santa Clara, CA) 6460 triple-quadrupole LC/MS/MS system. The precursor and product ions monitored via electrospray ionization in the positive ion mode with multiple reaction monitoring (MRM) as in **table S10**. Mass spectrometer parameter settings were gas temp (350 °C), gas flow (12 L/min), nebulizer (35 psi), sheath gas temp (400 °C), sheath gas

flow (12 L/min), capillary voltage (4,000v), and nozzle voltage (500v). Separation by liquid chromatography was achieved with a strong cation exchange column (Luna 5u SCX, 50 mm x 2.0 mm internal diameter) from Phenomenex (Torrance, CA) at 40 °C with 30 mM ammonium acetate in H_2O (solvent A) and 5% acetic acid in H_2O (solvent B). Two consecutive isocratic elution steps were employed starting with solvent A:B 12.5:87.5 held for 6 min. Then switched to 100% solvent A within 1 min and held for 4 min. Then back to initial composition and held constant for 3 min. The flow rate was 0.4 mL/min.

General procedure for hydrogenation of digoxin, digitoxin, digoxigenin, and ouabain

The hydrogenation procedure was adapted from conditions used previously for the reductions of digoxin (*19*), digitoxin (*20, 21*), digoxigenin (*22*), and ouabain (*23*). To a solution of substrate (50 mg; see *Bacterial strains and culturing conditions* for starting material supplier information) in a mixture of ethanol (4 mL) and 1,4-dioxane (2 mL) under a nitrogen atmosphere was added platinum(IV) oxide (15 mg). The reaction mixture was placed under a hydrogen atmosphere by evacuating the headspace of the reaction flask and then backfilling with a hydrogen-filled balloon (2 cycles). After stirring for 24 hours under an atmosphere of hydrogen, the reaction mixture was diluted with methanol (10 mL) and filtered through a pad of Celite. The Celite was washed with additional methanol (25 mL), and the combined filtrates were concentrated *in vacuo* using a rotary evaporator and then dried on a vacuum line to afford the hydrogenated product. Formation of fully hydrogenated material was confirmed using ^{1}H NMR spectra (**fig. S8**) and high-resolution mass spec (HRMS) (**fig. S9**).

NMR and HRMS

All chemicals and solvents used were obtained from Sigma-Aldrich except for CD_3OD, which was purchased from Cambridge Isotope Laboratories. NMR spectra were visualized using NUTS NMR Data Processing Software (Acorn NMR). ^{1}H NMR spectra were recorded on Varian INOVA 600 (600 MHz) NMR spectrometer at 23 ºC. Proton chemical shifts are referenced to residual protium in the NMR solvent (CD_3OD, 3.31 ppm). High-resolution mass spectral data for the synthetic hydrogenated products were

obtained at the small molecule mass spectrometry facility at Harvard University. An Agilent 6220 electrospray time-of-flight (ESI-TOF) mass spectrometer was used in positive ion mode. This instrument is equipped with a dual spray configuration and reference ions are introduced through a secondary nebulizer for internal calibration to get the highest possible mass accuracy and to correct for real-time drift in m/z values. Samples were introduced using an Agilent 1100 HPLC running at 250 μL/minute with 49:49:0.1% (v/v/v) water: acetonitrile: formic acid. The mass spectra were recorded between 100-3000 m/z. An m/z scale calibration using the Low Concentration Agilent Tune Mix (part number G1969-85000) was done immediately prior to analysis, and the m/z scale was corrected using the accurate mass of the reference ion at m/z 922.0 introduced through the secondary nebulizer.

Statistical analysis

Statistical significance was calculated by Student's *t* test, ANOVA, Wilcoxon matched-pairs signed rank test, or Mann-Whitney test as indicated. Analyses were performed using GraphPad Prism v5.0d (GraphPad Software, San Diego, CA) and Matlab version 7.12.0.

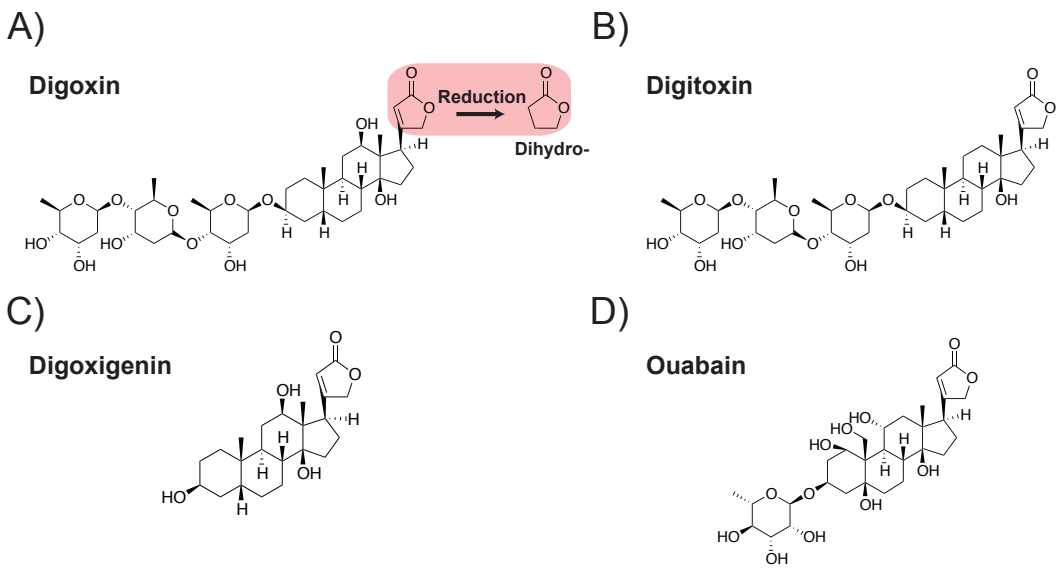

Fig. S1. Cardiac glycoside structures. Chemical structures of (A) digoxin, (B) digitoxin, (C) digoxigenin, and (D) ouabain with an α,β-unsaturated butyrolactone ring. The dihydro- variant of each compound contains a reduced butyrolactone ring as shown for digoxin.

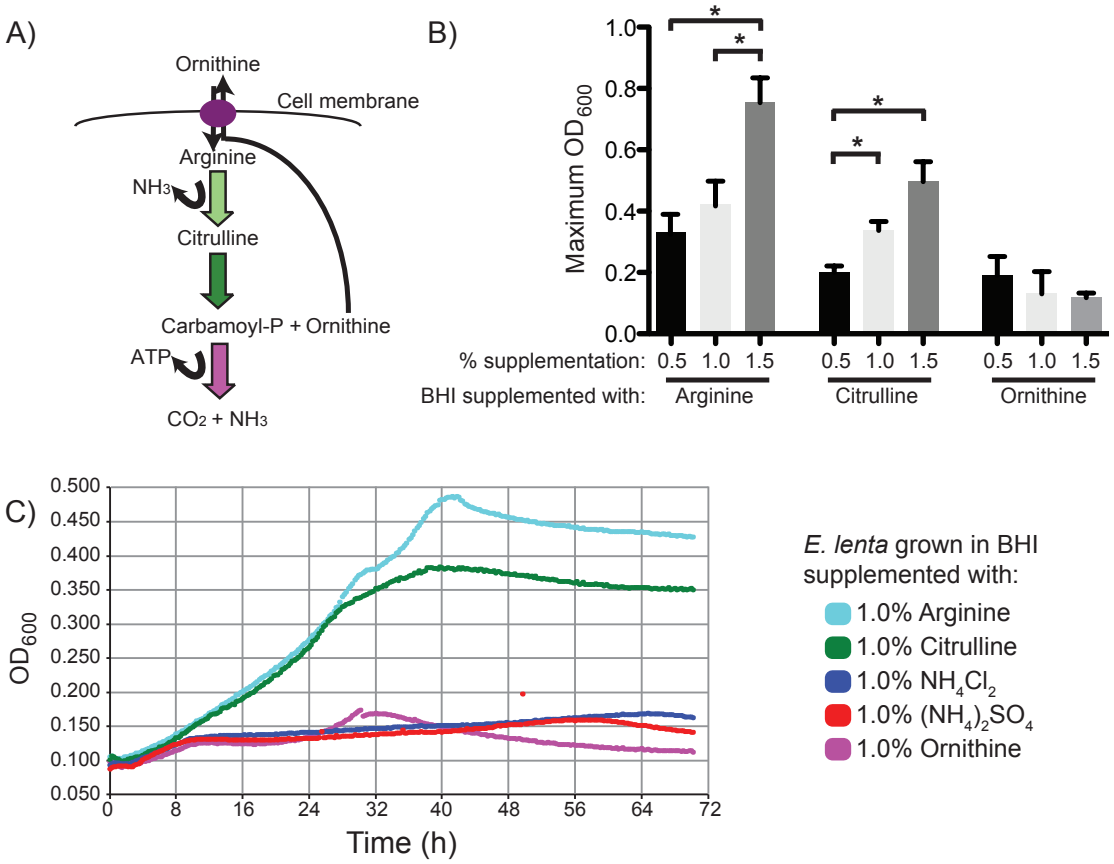

Fig. S2. The arginine dihydrolase pathway. (A) This pathway enables *E. lenta* to generate carbon, nitrogen, and energy from arginine. (B) The mean maximum OD_{600} reached when *E. lenta* is grown in BHI supplemented with arginine, citrulline, or ornithine. Values are the mean±sem. Asterisks represent statistical significance by Student's *t* test ($P<0.05$). (C) Representative growth curves of *E. lenta* growing in BHI supplemented with 1.0% of either: arginine, citrulline, NH_4Cl_2, $(NH_4)_2SO_4$, or ornithine. We did not detect an increase in the *in vitro* growth rate or carrying capacity in the presence of digoxin (**Fig. S3**), suggesting that this reduction may be an off-target reaction or only provide a fitness advantage under specific conditions.

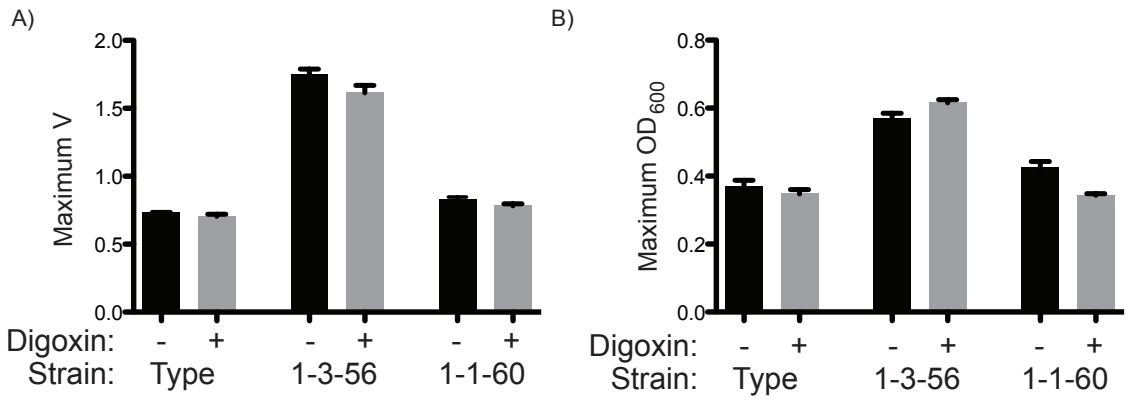

Fig. S3. Digoxin does not stimulate the growth of *E. lenta*. Comparison of growth rate (A) and maximum OD_{600} (B) of three *E. lenta* strains grown in BHI broth, in the presence and absence of 10 μg/mL digoxin. Values are the mean±sem. n=3 biological replicates/group. No significant differences were observed.

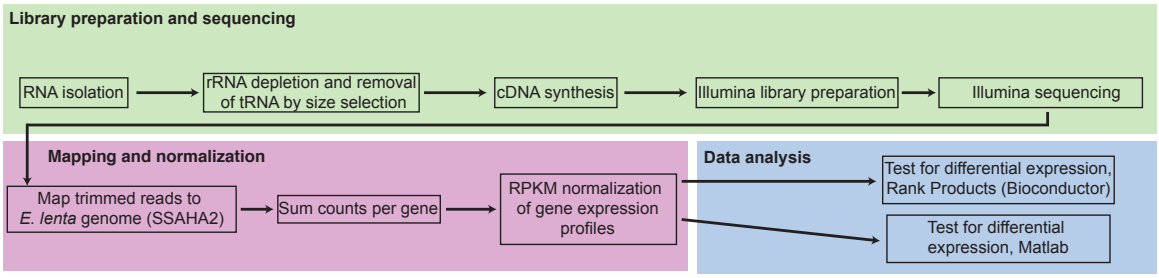

Fig. S4. Diagram of our RNA-Seq sample preparation and analysis pipeline. Samples from both exponential and early stationary phase were collected from triplicate cultures prior to library construction and high-throughput sequencing (*7*).

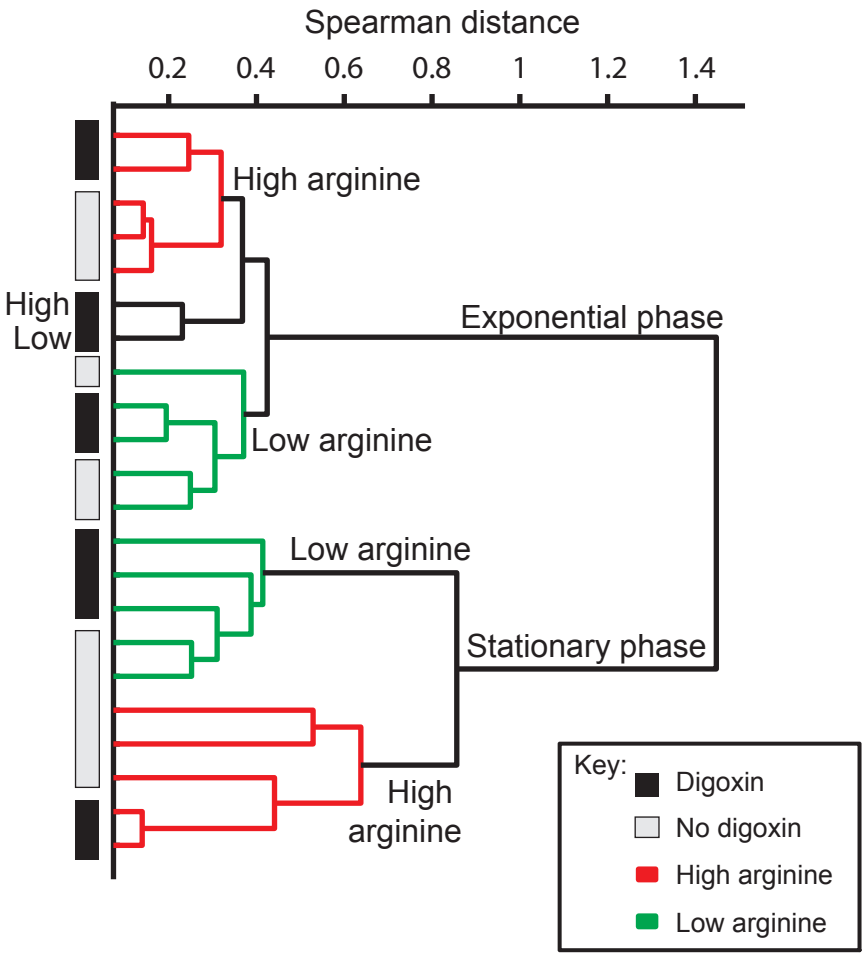

Fig. S5. *E. lenta* transcriptional profiles cluster according to growth phase, concentration of arginine, and then digoxin. Each gene's expression value was normalized by *z*-score prior to constructing a Spearman rank correlation distance matrix, UPGMA clustering, and display in dendrogram format (Matlab version 7.7.0). Branches are labeled by arginine concentration: green (low) and red (high). Tips are labeled by the presence (black) or absence (grey) of digoxin. We detected 1,136 genes differentially expressed in exponential relative to stationary phase, 22 genes affected by arginine during exponential growth, and 2,222 genes altered by arginine levels in stationary phase (**table S2**). These trends were confirmed by an independent Rank Products analysis (**table S3**).

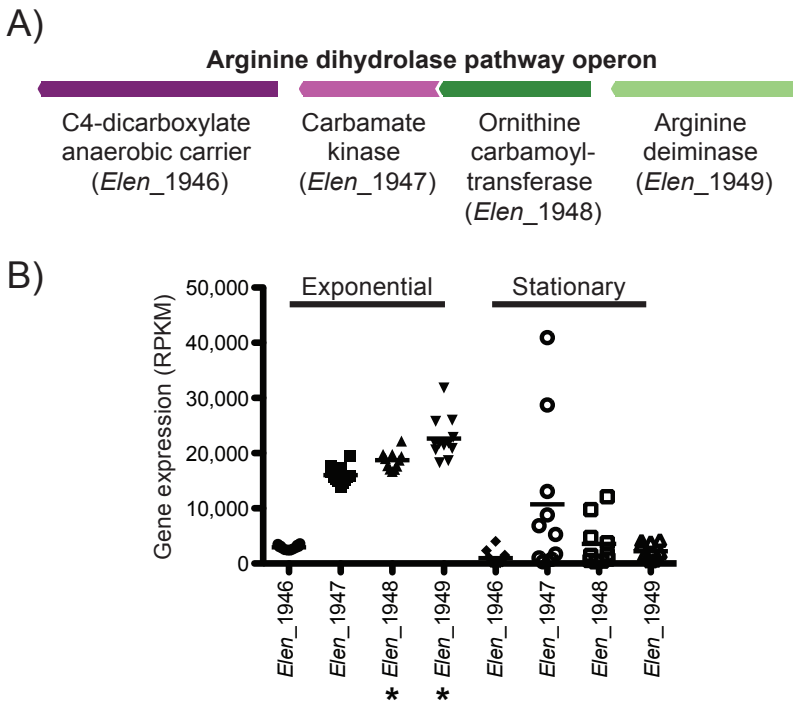

Fig. S6. The arginine dihydrolase operon is highly expressed in exponential phase. (A) A single operon, spanning *Elen*_1946 to *Elen*_1949 encodes all 3 enzymes and a putative arginine-ornithine antiporter (see **fig. S2A**). (B) All 4 genes in the arginine dihydrolase pathway operon were highly expressed during exponential growth, whereas the genes encoding the final two steps were significantly down-regulated in stationary phase. All values are shown (n=10-12 biological replicates/group), and lines represent the mean. Asterisks represent significant differences between exponential and stationary phase by ANOVA ($P<0.001$).

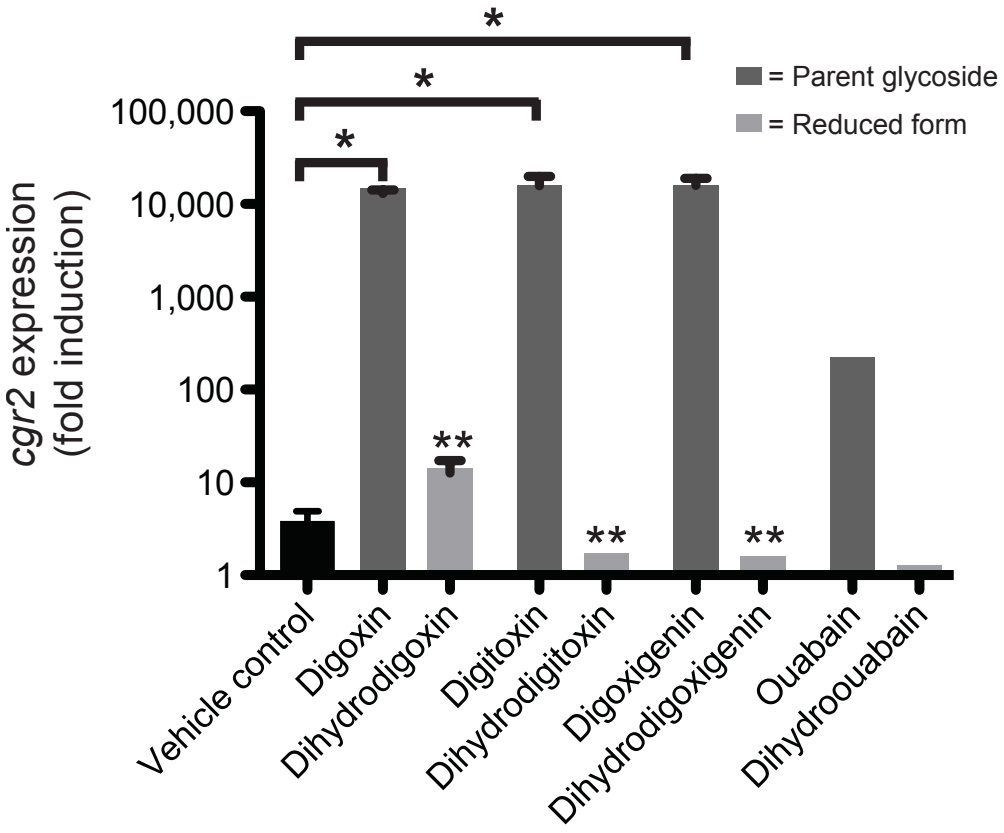

Fig. S7. Induction by related cardiac glycosides. The *cgr* operon is induced by cardiac glycosides containing unsaturated butyrolactone rings. qRT-PCR results are fold-changes, relative to the 16S rRNA transcript using the $2^{-\Delta\Delta Ct}$ method. Statistical significance was determined by ANOVA (*P<0.05; **P<0.01); n=2-3 biological replicates/compound. The most structurally distinct compound, ouabain, induced the *cgr* operon to significantly lower levels relative to digoxin (P<0.01, Student's *t* test).

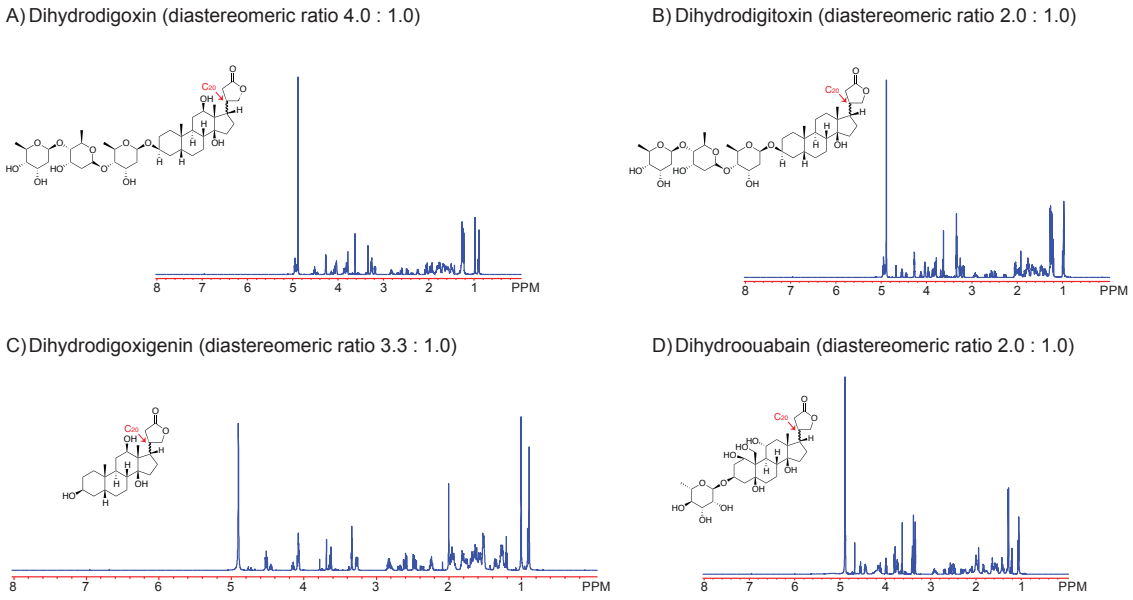

Fig. S8. NMR confirmation of reduced cardiac glycosides. ^{1}H NMR spectra (600 MHz) of hydrogenated digoxin (A), digitoxin (B), digoxigenin (C), and ouabain (D) in CD_3OD. The absence of the substrate alkene proton, which resonates between 5.5 - 6.0 ppm, indicated complete hydrogenation. All reactions provided reduced material as a mixture of two diastereomers, differing only in the configuration at C20 of the steroid scaffold.

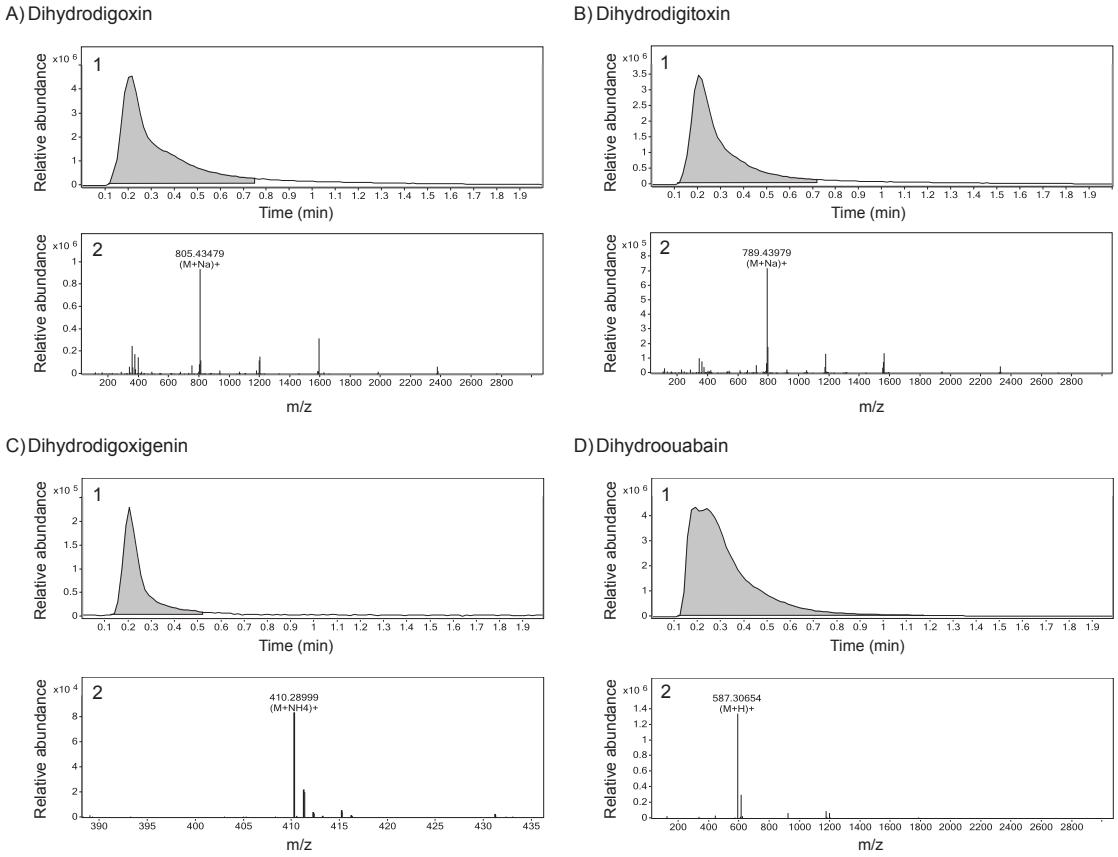

Fig. S9. High-resolution mass spectral data for synthetic hydrogenated products. 1: Total ion current and 2: mass spectrometry analysis of the corresponding signal. (A) Dihydrodigoxin: calculated for $C_{41}H_{66}NaO_{14}^{+}$ $[M+Na]^{+}$, 805.43448; found, 805.43479. (B) Dihydrodigitoxin: calculated for $C_{41}H_{66}NaO_{13}^{+}$ $[M+Na]^{+}$, 789.43956; found, 789.43979. (C) Dihydrodigoxigenin: calculated for $C_{23}H_{40}NO_{5}^{+}$ $[M+NH_4]^{+}$, 410.2901; found, 410.28999. (D) Dihydroouabain: calculated for $C_{29}H_{47}O_{12}^{+}$ $[M+H]^{+}$, 587.3062; found, 587.30654.

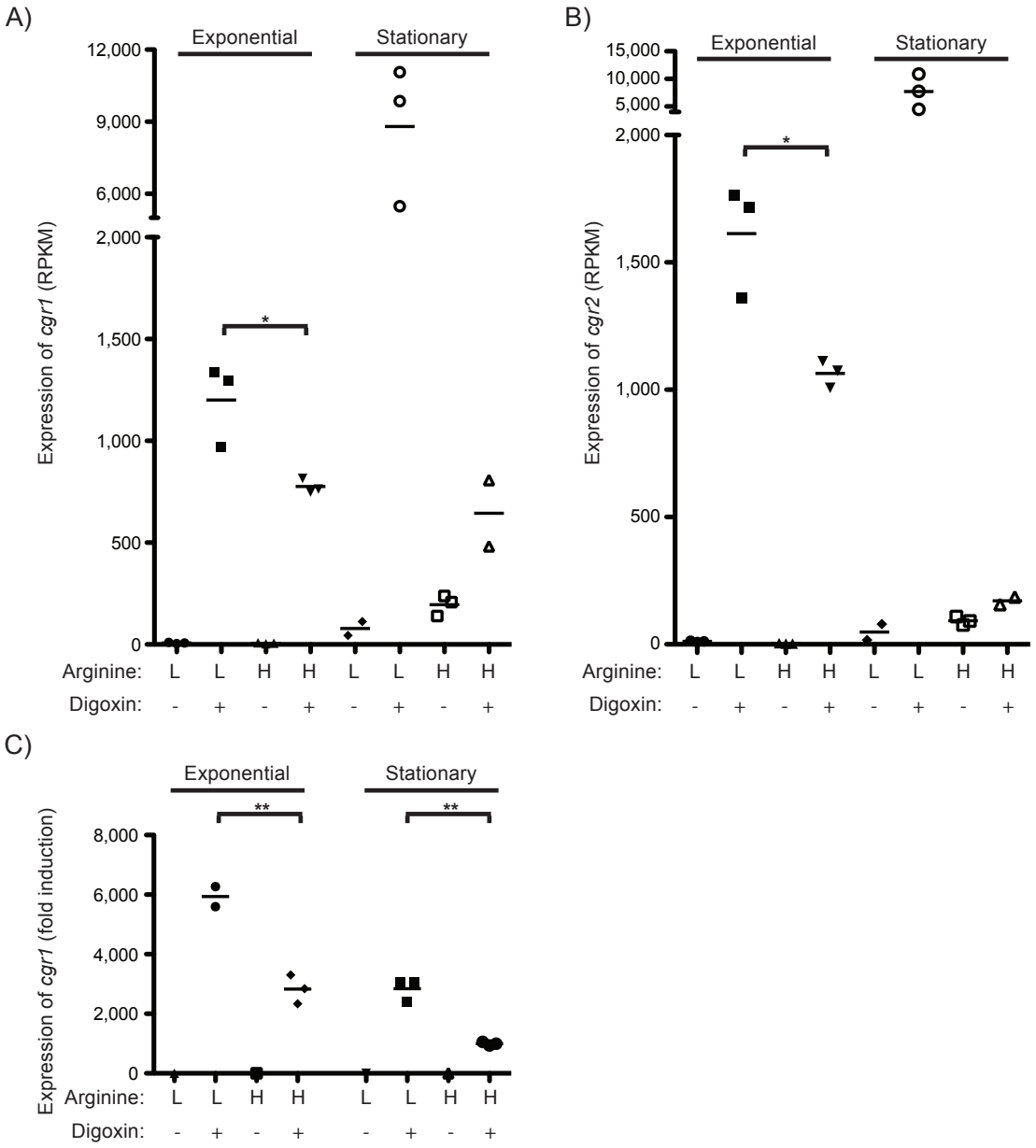

Fig. S10. High arginine levels limit the induction of the *cgr* operon. Normalized transcriptional levels (RPKM) are shown across growth phase, arginine levels, and digoxin for both genes in the *cgr* operon. Lines represent the mean; n=2-3 biological replicates/group. *cgr1* (A) and *cgr2* (B) transcription as determined by RNA-Seq. *cgr1* (C) transcription as determined by qRT-PCR. Asterisks indicate statistical significance by Student's *t* test (*=P<0.05; **=P<0.01).

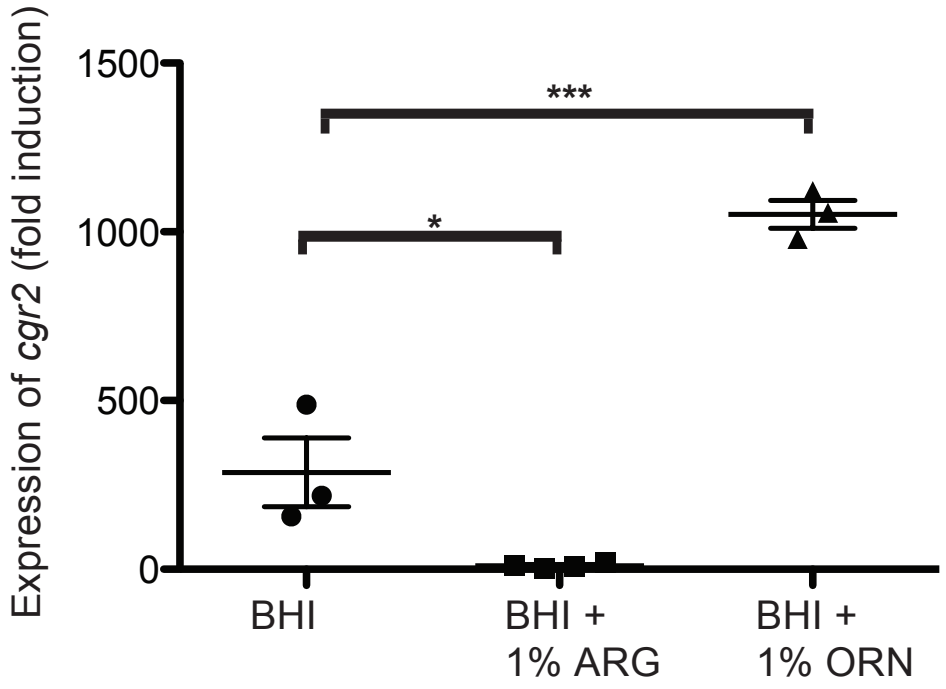

Fig. S11. *cgr2* transcription is repressed by arginine but not ornithine. qRT-PCR analysis of *cgr2* expression on cultures grown with BHI, BHI + 1% arginine, or BHI + 1% ornithine in the presence of digoxin. Asterisks indicate statistical significance by ANOVA (*=P<0.05; ***=P<0.001). Values are the mean±sem; n=3-4 biological replicates/group.

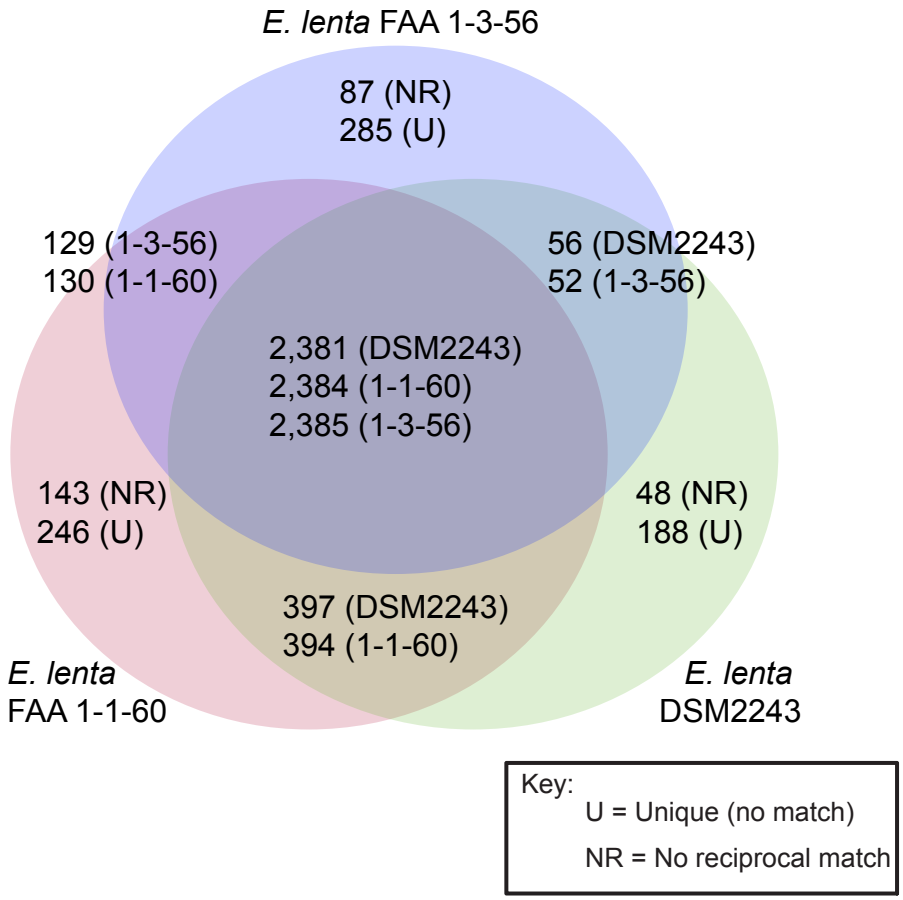

Fig. S12. Venn diagram of reciprocal BLASTP comparisons between 3 *E. lenta* genomes. The number of genes shared between each combination of genomes is shown in the overlapping sections, whereas each unique section is split between genes with significant homology but no reciprocal match (NR) and genes unique to each strain (U). Marker genes were highly conserved between strains: 16S rRNA (99.4% identity on average), 23S rRNA (99.7%), DNA gyrase A (99.6%), and DNA gyrase B (100.0%).

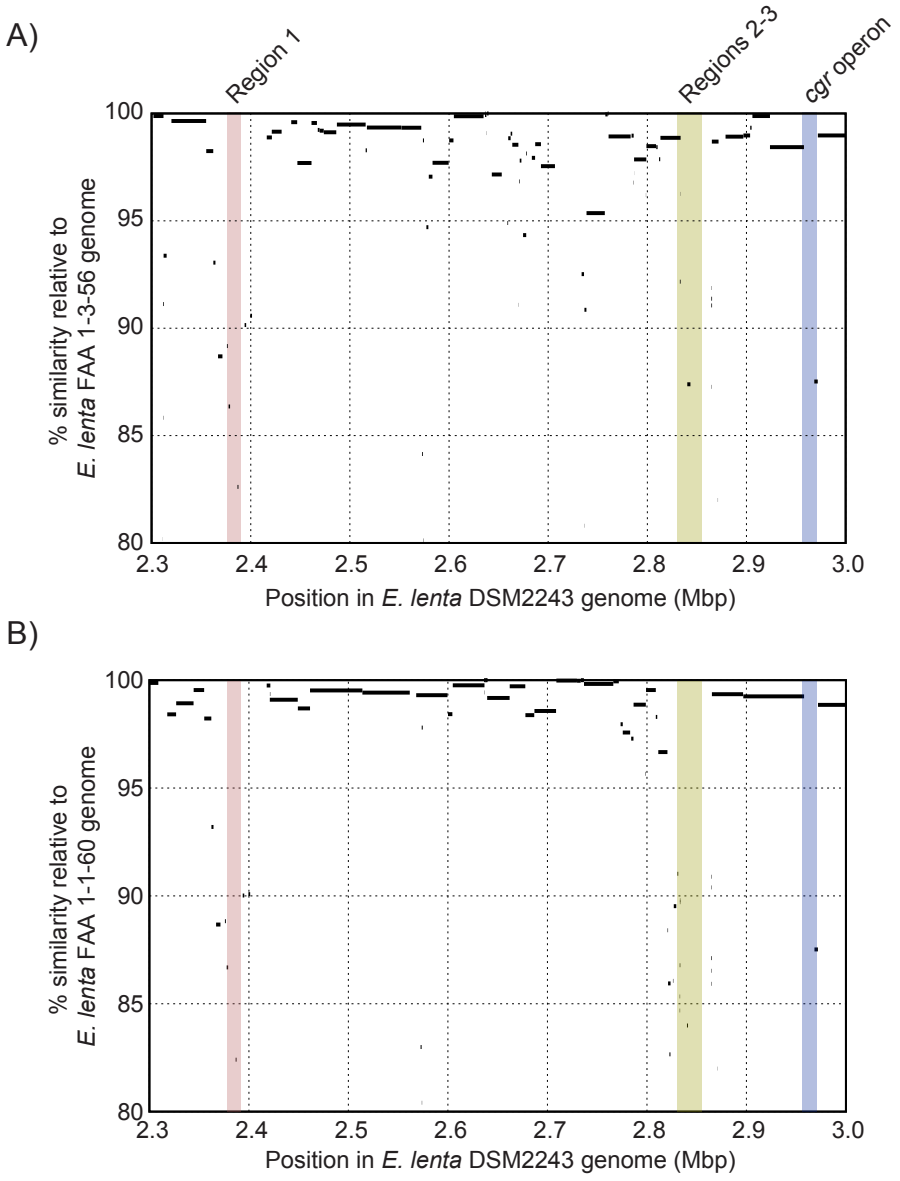

Fig. S13. The type strain contains multiple unique regions of interest. Whole genome sequence alignment of (A) the *E. lenta* FAA 1-3-56 draft assembly (28 scaffolds) and (B) the *E. lenta* FAA 1-1-60 draft assembly (44 scaffolds) to the *E. lenta* DSM2243 finished genome. Plots were generated using the MUMmer software package (*17*). The *cgr* operon and 3 other regions of interest are highlighted, representing genes up-regulated by digoxin and missing from the 2 non-reducing strains.

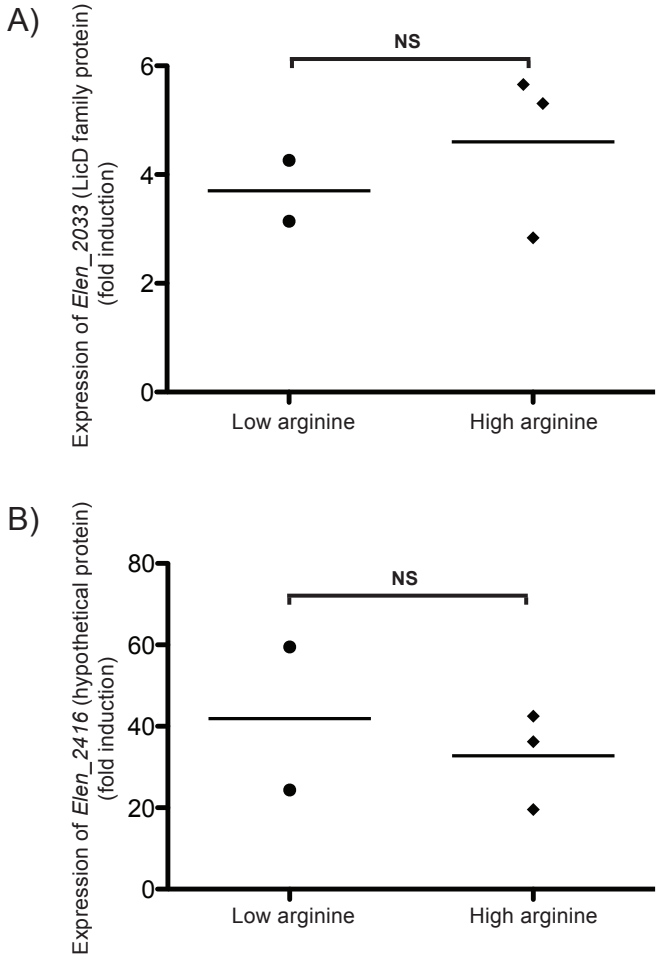

Fig. S14. Expression of the transporter-encoding genes unique to *E. lenta* DSM2243. Gene expression of (A) *Elen_2033*, and (B) *Elen_2416* was determined by qRT-PCR in low (0.25%) and high (1.25%) arginine conditions, with digoxin. Horizontal lines are the mean. See **table S4** for primer sequences. n=2-3 biological replicates/group; NS=not significant.

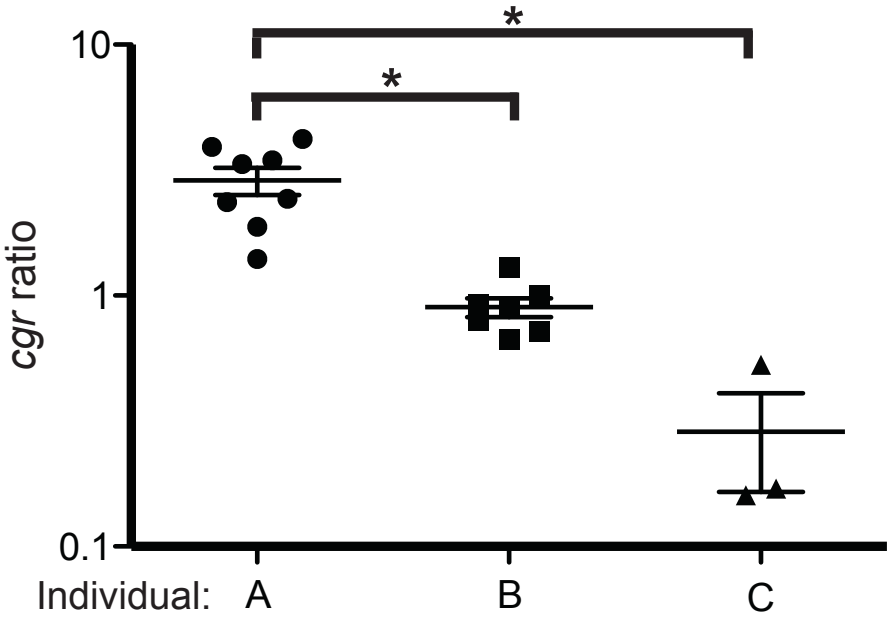

Fig. S15. The *cgr* ratio is stable over time. Samples from 3 unrelated individuals were collected over the course of 2-14 months (n=3-8 samples/individual). Asterisks indicate statistical significance by ANOVA ($P<0.05$). Values are the mean±sem.

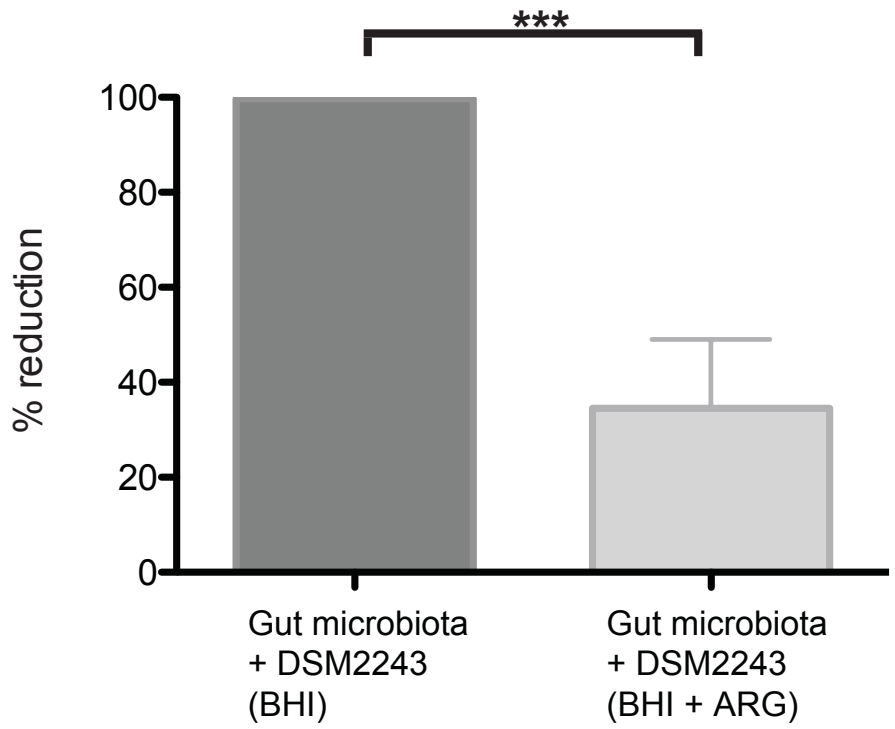

Fig. S16. Arginine prevents the gut microbiome plus *E. lenta* DSM2243 from reducing digoxin. Digoxin reduction is expressed as a percentage of the total drug amount, and was determined by LC/MS after 48 hours of growth. Values are the mean±sem. Statistical significance was determined by Student's *t* test ($P<0.001$; $n=3$). Error bars in left column are too small to visualize.

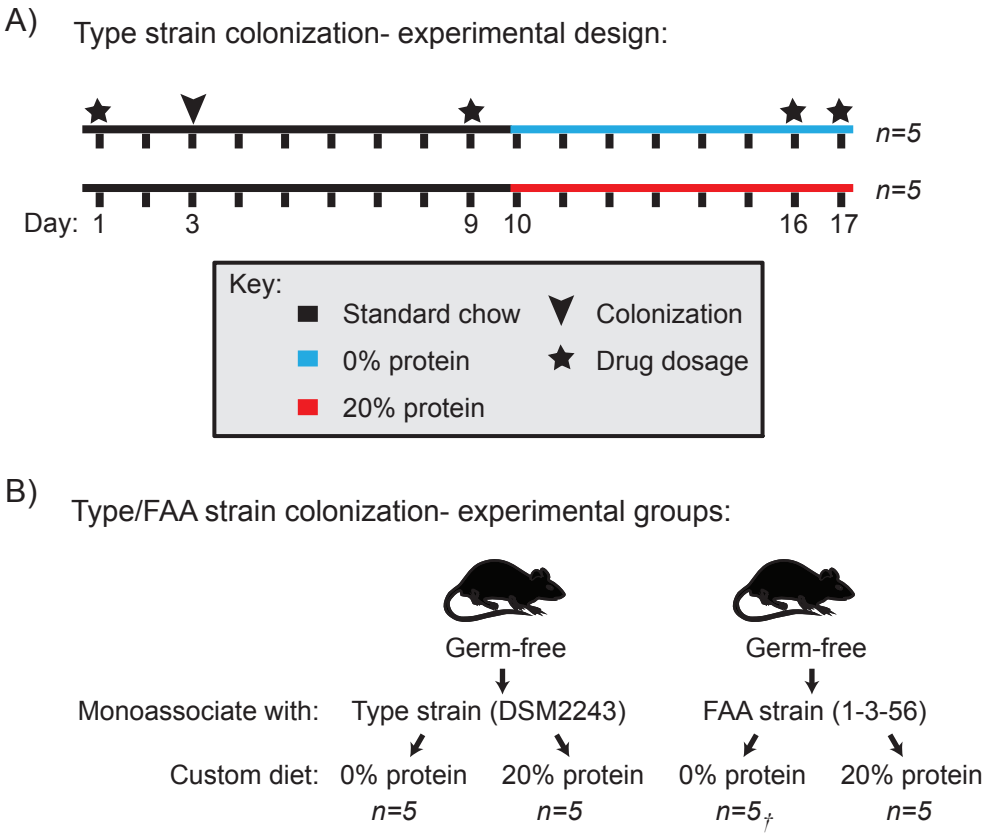

Fig. S17. Schematic diagrams for our mouse experiments. (A) Schematic diagram representing the first gnotobiotic mouse experiment: colonization by the *E. lenta* DSM2243 type strain. (B) Schematic diagram representing the second gnotobiotic mouse experiment: comparison of the impact of reducing and non-reducing strains of *E. lenta*. The timeline for the second experiment mirrored that of the first, except the number of days on the custom diet was reduced by one. '†' indicates that the original group size of n=5 was reduced to n=4 after one animal was sacrificed because of a health issue. Digoxin was orally administered at four different time-points: (i) prior to colonization, (ii) on the standard chow diet, (iii) after consumption of each defined diet, and (iv) before sacrifice.

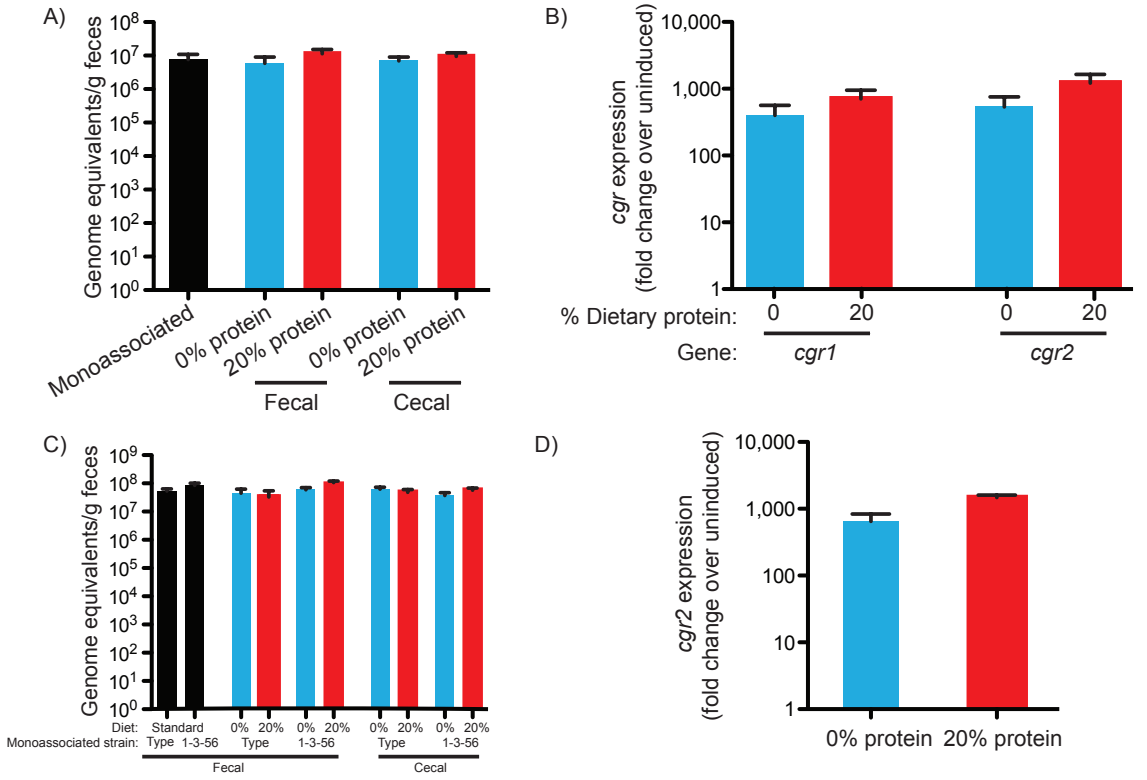

Fig. S18. Colonization and *cgr* operon expression in gnotobiotic mice. During the type strain monoassociation mouse experiment, *E. lenta* colonization was confirmed by measuring 16S rRNA gene levels in DNA extracted from fecal or cecal samples as indicated. Colonization under all conditions was significantly above the signal obtained from the germ-free background (9.7e3±2.6e3; P<0.05, Student's *t* test) (A). During this experiment *cgr* gene expression was measured by qRT-PCR using cecal contents as the starting material (B). Colonization levels for type/FAA 1-3-56 mouse experiment were also significantly above the germ-free background (8.0e5±1.7e5; P<0.05, Student's *t* test) (C); *cgr* gene expression was determined as in the previous mouse experiment (D). Values are the mean±sem. n=4 or 5 per group, see **fig. S17**.

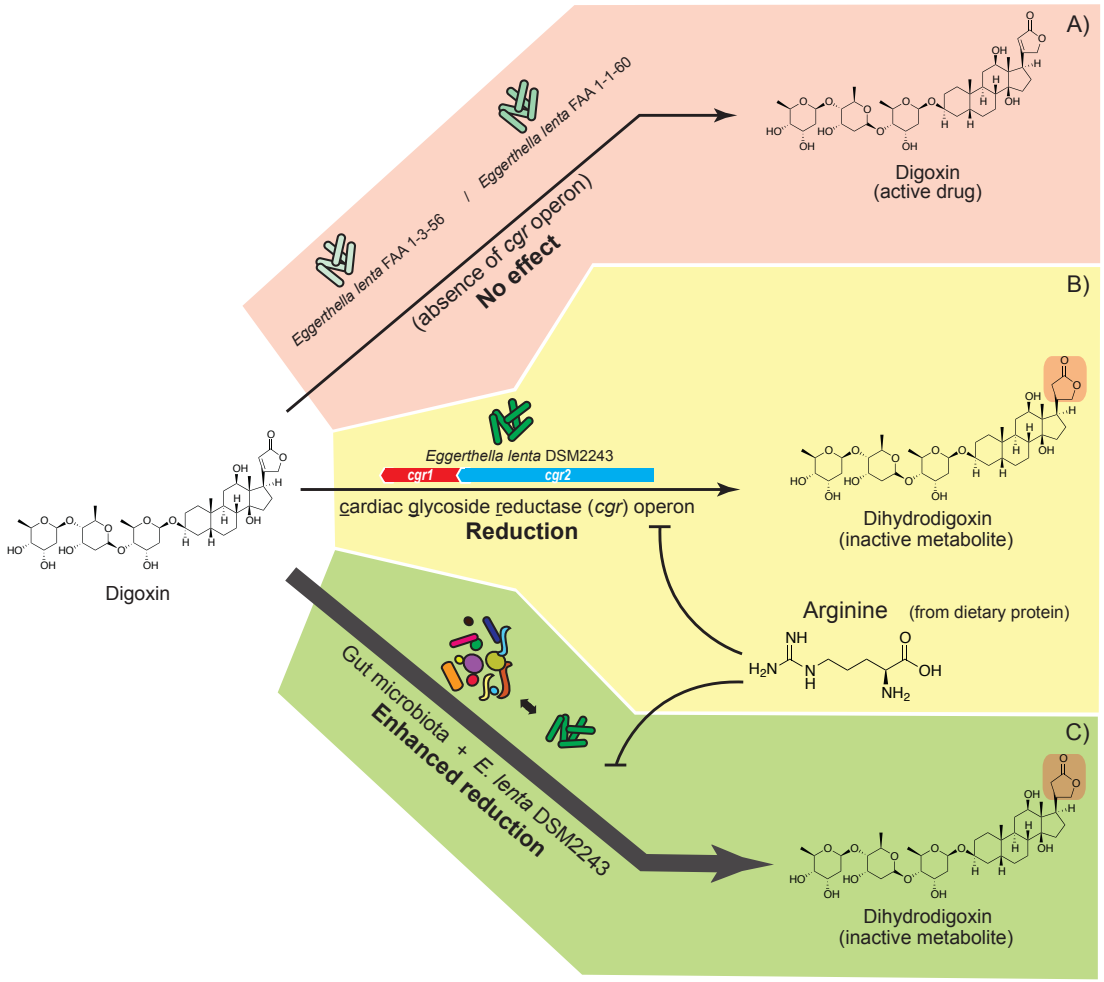

Fig. S19. A model for how strain-level variation, community structure, and host diet affects drug inactivation. Individuals are colonized by a mixture of *E. lenta* strains. Strains such as FAA 1-3-56 and 1-1-60 have no impact on the metabolism of digoxin (A). The DSM2243 strain however, has the ability to transform digoxin to the cardioinactive metabolite, dihydrodigoxin; reduction capability is encoded by the *cgr* operon (B). Digoxin inactivation is inhibited by arginine originating from dietary protein (B,C). Interactions between *E. lenta* and other members of the gut microbiome can increase digoxin reduction efficiency (C).

Table S1. RNA-Seq statistics.

Table S2A-D. Standard analysis of RNA-Seq data. Genes differentially expressed between (A) exponential and stationary phase growth, (B) high and low arginine during exponential growth, (C) high and low arginine during stationary phase, and (D) with or without digoxin during exponential growth.

Table S3A-I. Rank products analysis of RNA-Seq data. Genes differentially expressed between (A) exponential and stationary phase growth, (B) high and low arginine during exponential growth, (C) high and low arginine during stationary phase, (D) with or without digoxin during exponential growth, (E) with or without digoxin during exponential growth in low arginine, (F) with or without digoxin during exponential growth in high arginine, (G) with or without digoxin during stationary phase, (H) with or without digoxin during stationary phase in low arginine, and (I) with or without digoxin during stationary phase in high arginine.

Table S4. *E. lenta* specific primers used for quantitative PCR.

Table S5. Clinical usage, and bioavailability information for digoxin, digoxigenin, digitoxin (*24*) and ouabain (*25*).

Table S6. Genes unique to the *E. lenta* DSM2243 genome.

Table S7. Diet information for mouse experiments.

Table S8. Chow consumption and weight data from mouse experiments.

Table S9. Analysis of ileal amino acid content. Amino acids were quantified from ileal samples from *E. lenta* monoassociated mice (n=3/diet group).

Table S10. Multiple reaction monitoring parameters for amino acid analysis.

Table S1. RNA-seq statistics

Sample	Barcode Sequence	Sequencing pool	Growth phase	Arginine concentration	Digoxin	Raw sequences	Filtered sequences	% reads mapped	% 16S rRNA	% 23S rRNA	% coding sequences
EL11	ATCACG	1	Stationary	0.25	N	1,789,425	1,785,821	99.3	11.3	85.3	1.8
EL13	TTAGGC	1	Stationary	0.25	N	1,806,486	1,803,057	98.9	11.2	82.5	3.2
EL14	TGACCA	1	Stationary	0.25	Y	2,010,344	2,006,356	99.4	11.2	85.8	1.0
EL15	ACAGTG	1	Stationary	0.25	Y	1,906,517	1,902,596	99.3	10.5	84.6	2.4
EL16	GCCAAT	1	Stationary	0.25	Y	2,294,937	2,290,401	99.1	10.3	82.6	5.0
EL17	CAGATC	1	Stationary	1.25	N	1,814,146	1,810,416	99.4	14.1	84.8	0.2
EL18	ACTTGA	1	Stationary	1.25	N	1,716,501	1,713,074	99.2	11.9	85.8	0.5
EL19	GATCAG	1	Stationary	1.25	N	1,855,878	1,851,949	99.4	10.1	87.7	0.7
EL20	TAGCTT	1	Stationary	1.25	Y	1,956,758	1,952,702	99.6	13.2	86.0	0.0
EL22	CTTGTA	1	Stationary	1.25	Y	4,319	4,306	98.5	10.0	84.0	3.8
EL23	ATCACG	2	Exponential	0.25	N	1,080,486	1,077,086	96.4	9.7	57.4	32.0
EL24	CGATGT	2	Exponential	0.25	N	1,013,603	1,010,128	96.7	8.8	54.4	35.4
EL25	TTAGGC	2	Exponential	0.25	N	1,390,127	1,385,743	96.8	9.2	54.3	35.4
EL26	TGACCA	2	Exponential	0.25	Y	1,856,687	1,850,601	95.5	8.2	41.7	49.7
EL27	ACAGTG	2	Exponential	0.25	Y	1,856,559	1,850,510	96.1	7.7	43.2	48.4
EL28	GCCAAT	2	Exponential	0.25	Y	2,188,400	2,181,905	96.7	9.6	52.5	36.7
EL29	CAGATC	2	Exponential	1.25	N	1,572,925	1,568,089	96.2	8.5	49.3	41.5
EL30	ACTTGA	2	Exponential	1.25	N	2,181,628	2,174,846	96.3	8.6	49.5	41.1
EL31	GATCAG	2	Exponential	1.25	N	1,577,772	1,572,782	96.7	9.8	55.5	33.5
EL32	TAGCTT	2	Exponential	1.25	Y	2,021,335	2,014,775	95.7	9.4	44.0	46.1
EL33	GGCTAC	2	Exponential	1.25	Y	1,157,122	1,153,525	96.3	13.1	59.2	26.4
EL34	CTTGTA	2	Exponential	1.25	Y	1,494,875	1,490,157	95.9	10.6	50.6	38.0

Stationary	**Mean**	1,715,531	1,712,068	99.21	11.38	84.90	1.85
	SEM	196,884	196,488	0.10	0.43	0.50	0.54
Exponential	**Mean**	1,615,960	1,610,846	96.28	9.43	50.97	38.69
	SEM	118,606	118,248	0.12	0.40	1.64	2.01

Table S2.(A) Genes up-regulated in exponential growth relative to stationary phase (FDR<0.01, >10-fold change)

Gene identity	Fold-change
Elen_0706_CDS_acetate/CoA_ligase	144.58
Elen_1838_CDS_Aldehyde_Dehydrogenase	94.75
Elen_0707_CDS_hypothetical_protein	68.99
Elen_2143_CDS_pyruvate_ferredoxin/flavodoxin_oxidoreductase	45.65
Elen_2145_CDS_extracellular_solute-binding_protein_family_5	30.26
Elen_2781_CDS_glutamate_synthase_(NADPH),_homotetrameric	28.71
Elen_1570_CDS_NADH_dehydrogenase_(quinone)	27.68
Elen_1325_CDS_short-chain_dehydrogenase/reductase_SDR	27.48
Elen_1573_CDS_hypothetical_protein	27.15
Elen_1276_CDS_nickel-dependent_hydrogenase_large_subunit	25.16
Elen_1224_CDS_extracellular_solute-binding_protein_family_5	23.18
Elen_2782_CDS_oxidoreductase_FAD/NAD(P)-binding_domain_protein	22.65
Elen_1275_CDS_hydrogenase_(NiFe)_small_subunit_HydA	22.37
Elen_1574_CDS_NADH_dehydrogenase_(quinone)	21.96
Elen_0690_CDS_short-chain_dehydrogenase/reductase_SDR	21.77
Elen_0753_CDS_diaminopimelate_dehydrogenase	21.17
Elen_1682_CDS_molydopterin_dinucleotide-binding_region	20.80
Elen_1729_CDS_acetate_kinase	20.21
Elen_1563_CDS_Endoribonuclease_L-PSP	18.85
Elen_0014_CDS_PpiC-type_peptidyl-prolyl_cis-trans_isomerase	17.54
Elen_1896_CDS_thioredoxin	17.51
Elen_0740_CDS_hypothetical_protein	16.68
Elen_1256_CDS_nickel-dependent_hydrogenase_large_subunit	16.56
Elen_1779_CDS_glyceraldehyde-3-phosphate_dehydrogenase,_type_I	16.22
Elen_1043_CDS_ATP_synthase_F1,_alpha_subunit	14.59
Elen_1255_CDS_NADH_ubiquinone_oxidoreductase_20_kDa_subunit	14.18
Elen_1253_CDS_4Fe-4S_ferredoxin,_iron-sulfur_binding_domain_protein	13.90
Elen_0715_CDS_DNA-directed_RNA_polymerase,_beta_subunit	12.90
Elen_1236_CDS_Dinitrogenase_iron-molybdenum_cofactor_biosynthesis_protein	12.53
Elen_1044_CDS_ATP_synthase_F1,_gamma_subunit	12.18
Elen_2270_CDS_FeS_assembly_ATPase_SufC	12.00
Elen_2896_CDS_ATP-dependent_metalloprotease_FtsH	11.76
Elen_1254_CDS_oxidoreductase_FAD/NAD(P)-binding_domain_protein	11.15
Elen_1571_CDS_respiratory-chain_NADH_dehydrogenase_subunit_1	10.90
Elen_2337_CDS_glycosyl_transferase_family_51	10.87
Elen_1681_CDS_4Fe-4S_ferredoxin_iron-sulfur_binding_domain_protein	10.29
Elen_1045_CDS_ATP_synthase_F1,_beta_subunit	10.25
Elen_1277_CDS_cytochrome_B561	10.23
Elen_2541_CDS_acetyl-CoA_carboxylase,_biotin_carboxylase	10.18
Elen_1949_CDS_arginine_deiminase	10.12
Elen_1778_CDS_Phosphoglycerate_kinase	10.10

Table S2.(B) Genes differentially expressed during exponential growth in high versus low arginine (FDR<0.05, >2-fold change)

Gene identity	Fold-change*
Elen_0706_CDS_acetate/CoA_ligase	3.03
Elen_2438_CDS_hypothetical_protein	2.63
Elen_2872_CDS_Electron_transfer_flavoprotein_alpha_subunit	2.54
Elen_0443_CDS_4Fe-4S_ferredoxin_iron-sulfur_binding_domain_protein	2.54
Elen_2397_CDS_protein_of_unknown_function_DUF901	2.50
Elen_2440_CDS_LicD_family_protein	2.47
Elen_2898_CDS_maf_protein	2.45
Elen_0438_CDS_protein_of_unknown_function_DUF218	2.36
Elen_2269_CDS_transcriptional_regulator,_BadM/Rrf2_family	2.34
Elen_0439_CDS_Asp/Glu/hydantoin_racemase	2.34
Elen_2350_CDS_peptidylprolyl_isomerase_FKBP-type	2.32
Elen_0440_CDS_transcriptional_regulator,_LuxR_family	2.28
Elen_2002_CDS_protein_of_unknown_function_DUF497	2.24
Elen_2374_CDS_Nitrate_reductase	2.17
Elen_0429_CDS_hypothetical_protein	2.04
Elen_2909_CDS_LrgB_family_protein	2.04
Elen_1573_CDS_hypothetical_protein	-2.00
Elen_1572_CDS_NADH_ubiquinone_oxidoreductase_20_kDa_subunit	-2.13
Elen_2941_CDS_peptidase_S8_and_S53_subtilisin_kexin_sedolisin	-2.15
Elen_0694_CDS_electron_transport_complex,_RnfABCDGE_type,_B_subunit	-3.52
Elen_0695_CDS_electron_transport_complex,_RnfABCDGE_type,_A_subunit	-3.53
Elen_0696_CDS_electron_transport_complex,_RnfABCDGE_type,_E_subunit	-4.27

*Positive fold-change indicates up-regulation in high arginine.

Table S2.(C) Genes differentially expressed during stationary phase in high versus low arginine (FDR<0.05, >10-fold change)

Gene identity	Fold-change*
Elen_1880_CDS_NusG_antitermination_factor	73.31
Elen_1186_CDS_major_facilitator_superfamily_MFS_1	29.66
Elen_1190_CDS_molybdopterin_oxidoreductase	22.80
Elen_3011_CDS_SNARE_associated_Golgi_protein	17.05
Elen_2273_CDS_cysteine_desulfurase,_SufS_subfamily	16.82
Elen_1879_CDS_Undecaprenyl-phosphate_galactose_phosphotransferase	16.65
Elen_0107_CDS_flavocytochrome_c	16.36
Elen_2718_CDS_major_facilitator_superfamily_MFS_1	16.02
Elen_3010_CDS_histidine_kinase	15.45
Elen_1806_CDS_riboflavin_biosynthesis_protein_RibF	14.54
Elen_2272_CDS_SufBD_protein	13.95
Elen_0285_CDS_heat_shock_protein_DnaJ_domain_protein	13.77
Elen_3101_CDS_L-carnitine_dehydratase/bile_acid-inducible_protein_F	13.05
Elen_1195_CDS_hypothetical_protein	12.63
Elen_0497_CDS_molydopterin_dinucleotide-binding_region	12.57
Elen_2580_CDS_cytochrome_c_assembly_protein	12.44
Elen_1193_CDS_hypothetical_protein	12.41
Elen_2719_CDS_beta-lactamase_domain_protein	11.98
Elen_1201_CDS_Galactokinase	11.81
Elen_2284_CDS_Bile_acid:sodium_symporter	11.65
Elen_2548_CDS_3-dehydroquinate_synthase	11.52
Elen_2396_CDS_conserved_hypothetical_protein	11.16
Elen_3007_CDS_hypothetical_protein	11.13
Elen_1187_CDS_transcriptional_regulator,_MerR_family	10.98
Elen_3103_CDS_MaoC_domain_protein_dehydratase	10.98
Elen_1766_CDS_hypothetical_protein	10.80
Elen_1793_CDS_amino_acid_adenylation_domain_protein	10.78
Elen_1202_CDS_glycoside_hydrolase_family_2_sugar_binding	10.75
Elen_2433_CDS_conserved_hypothetical_protein	10.64
Elen_2757_CDS_fumarate_reductase/succinate_dehydrogenase_flavoprotein_doma	10.59
Elen_3006_CDS_Abortive_infection_protein	10.54
Elen_1194_CDS_hypothetical_protein	10.45
Elen_0558_CDS_cell_wall/surface_repeat_protein	10.43
Elen_2372_CDS_Polysulphide_reductase_NrfD	10.22
Elen_1336_CDS_protein_of_unknown_function_DUF512	10.04
Elen_2133_CDS_translation_elongation_factor_Tu	-10.66
Elen_2679_CDS_Glutathione_peroxidase	-10.77
Elen_2222_CDS_hypothetical_protein	-11.15
Elen_1124_CDS_flavin_reductase_domain_protein_FMN-binding	-11.87
Elen_2528_CDS_hypothetical_protein	-14.16
Elen_0146_CDS_General_substrate_transporter	-14.24
Elen_0297_CDS_hypothetical_protein	-14.51
Elen_0391_CDS_heat_shock_protein_Hsp20	-19.64
Elen_0153_CDS_arginine_deiminase	-22.55
Elen_1568_CDS_C4-dicarboxylate_anaerobic_carrier	-25.19
Elen_0398_CDS_Rubrerythrin	-35.36
Elen_2529_CDS_fumarate_reductase/succinate_dehydrogenase_flavoprotein_doma	-37.55
Elen_0128_CDS_Catalase	-37.98
Elen_0138_CDS_Rubrerythrin	-54.59

*Positive fold-change indicates up-regulation in high arginine.

Table S2.(D) Genes differentially expressed during exponential growth with or without digoxin (FDR<0.05, >2-fold change)

Gene identity	Fold-change*
Elen_2529_CDS_fumarate_reductase/succinate_dehydrogenase_flavoprotein_domain_protein	174.38
Elen_2528_CDS_hypothetical_protein	155.97
Elen_2728_CDS_RNA_polymerase,_sigma-24_subunit,_ECF_subfamily	3.72
Elen_2729_CDS_hypothetical_protein	2.81
Elen_2106_CDS_CTP_synthase	-2.02
Elen_2070_CDS_porphobilinogen_deaminase	-2.11
Elen_2071_CDS_glutamyl-tRNA_reductase	-2.12
Elen_1886_CDS_hypothetical_protein	-2.46
Elen_1291_CDS_transcriptional_regulator,_LuxR_family	-2.61
Elen_2586_CDS_Nitrite_reductase_(cytochrome;_ammonia-forming)	-2.86

*Positive fold-change indicates up-regulation with digoxin.

Table S3.(A) Genes up-regulated during exponential growth relative to stationary phase (Rank products analysis; % false predictions<0.05, >10-fold change)

Gene identity	Fold-change*
Elen_0706_CDS_acetate/CoA_ligase	144.93
Elen_1838_CDS_Aldehyde_Dehydrogenase	94.34
Elen_0707_CDS_hypothetical_protein	68.97
Elen_2143_CDS_pyruvate_ferredoxin/flavodoxin_oxidoreductase	45.66
Elen_2145_CDS_extracellular_solute-binding_protein_family_5	30.21
Elen_2781_CDS_glutamate_synthase_(NADPH),_homotetrameric	28.74
Elen_1570_CDS_NADH_dehydrogenase_(quinone)	27.70
Elen_1325_CDS_short-chain_dehydrogenase/reductase_SDR	27.47
Elen_1573_CDS_hypothetical_protein	27.17
Elen_1276_CDS_nickel-dependent_hydrogenase_large_subunit	25.19
Elen_1224_CDS_extracellular_solute-binding_protein_family_5	23.20
Elen_2782_CDS_oxidoreductase_FAD/NAD(P)-binding_domain_protein	22.68
Elen_1275_CDS_hydrogenase_(NiFe)_small_subunit_HydA	22.37
Elen_1574_CDS_NADH_dehydrogenase_(quinone)	21.98
Elen_0690_CDS_short-chain_dehydrogenase/reductase_SDR	21.79
Elen_0753_CDS_diaminopimelate_dehydrogenase	21.19
Elen_1682_CDS_molydopterin_dinucleotide-binding_region	20.79
Elen_1729_CDS_acetate_kinase	20.20
Elen_1563_CDS_Endoribonuclease_L-PSP	18.87
Elen_0014_CDS_PpiC-type_peptidyl-prolyl_cis-trans_isomerase	17.54
Elen_1896_CDS_thioredoxin	17.51
Elen_0740_CDS_hypothetical_protein	16.69
Elen_1256_CDS_nickel-dependent_hydrogenase_large_subunit	16.56
Elen_1779_CDS_glyceraldehyde-3-phosphate_dehydrogenase,_type_I	16.23
Elen_1043_CDS_ATP_synthase_F1,_alpha_subunit	14.60
Elen_1255_CDS_NADH_ubiquinone_oxidoreductase_20_kDa_subunit	14.18
Elen_1253_CDS_4Fe-4S_ferredoxin,_iron-sulfur_binding_domain_protein	13.91
Elen_0715_CDS_DNA-directed_RNA_polymerase,_beta'_subunit	12.90
Elen_1236_CDS_Dinitrogenase_iron-molybdenum_cofactor_biosynthesis_protein	12.53
Elen_1044_CDS_ATP_synthase_F1,_gamma_subunit	12.18
Elen_2270_CDS_FeS_assembly_ATPase_SufC	11.99
Elen_2896_CDS_ATP-dependent_metalloprotease_FtsH	11.76
Elen_1254_CDS_oxidoreductase_FAD/NAD(P)-binding_domain_protein	11.15
Elen_1571_CDS_respiratory-chain_NADH_dehydrogenase_subunit_1	10.89
Elen_2337_CDS_glycosyl_transferase_family_51	10.87
Elen_1681_CDS_4Fe-4S_ferredoxin_iron-sulfur_binding_domain_protein	10.29
Elen_1045_CDS_ATP_synthase_F1,_beta_subunit	10.25
Elen_1277_CDS_cytochrome_B561	10.24
Elen_2541_CDS_acetyl-CoA_carboxylase,_biotin_carboxylase	10.18
Elen_1949_CDS_arginine_deiminase	10.12
Elen_1778_CDS_Phosphoglycerate_kinase	10.10

Table S3.(B) Genes differentially expressed during exponential growth in high versus low arginine (Rank products analysis; % false predictions<0.05, >2-fold change)

Gene identity	Fold-change*
Elen_0558_CDS_cell_wall/surface_repeat_protein	3.44
Elen_0655_CDS_hypothetical_protein	3.36
Elen_0253_CDS_succinate_dehydrogenase_and_fumarate_reductase_iron-sulfur_protein	3.30
Elen_0425_CDS_cytoplasmic_chaperone_TorD_family_protein	3.04
Elen_0706_CDS_acetate/CoA_ligase	3.03
Elen_2438_CDS_hypothetical_protein	2.63
Elen_2872_CDS_Electron_transfer_flavoprotein_alpha_subunit	2.54
Elen_0441_CDS_hypothetical_protein	2.53
Elen_0019_CDS_hypothetical_protein	-2.04
Elen_0403_CDS_NLPA_lipoprotein	-2.06
Elen_0401_CDS_binding-protein-dependent_transport_systems_inner_membrane_component	-2.31
Elen_0703_CDS_response_regulator_receiver_protein	-2.31
Elen_0742_CDS_protein_of_unknown_function_DUF214	-2.39
Elen_0699_CDS_electron_transport_complex,_RnfABCDGE_type,_C_subunit	-2.42
Elen_1788_CDS_beta-lactamase	-2.42
Elen_1742_CDS_4Fe-4S_ferredoxin_iron-sulfur_binding_domain_protein	-2.45
Elen_0740_CDS_hypothetical_protein	-2.46
Elen_0792_CDS_NLP/P60_protein	-2.46
Elen_2223_CDS_RNA_polymerase,_sigma-24_subunit,_ECF_subfamily	-2.47
Elen_0316_CDS_ABC_transporter_related	-2.51
Elen_1739_CDS_molybdopterin_oxidoreductase	-2.55
Elen_2087_CDS_conserved_hypothetical_protein	-2.56
Elen_3050_CDS_4Fe-4S_ferredoxin_iron-sulfur_binding_domain_protein	-2.57
Elen_0500_CDS_transcriptional_regulator,_LuxR_family	-2.66
Elen_3051_CDS_molybdopterin_oxidoreductase	-2.66
Elen_1740_CDS_hypothetical_protein	-2.80
Elen_0739_CDS_hypothetical_protein	-2.88
Elen_1822_CDS_Electron-transferring-flavoproteindehydrogenase	-2.96
Elen_2354_CDS_fumarate_reductase/succinate_dehydrogenase_flavoprotein_domain_protein	-3.00
Elen_1741_CDS_NapD_family_protein	-3.04
Elen_2413_CDS_hypothetical_protein	-3.09
Elen_0741_CDS_ABC_transporter_related	-3.11
Elen_1792_CDS_membrane_bound_O-acyl_transferase_MBOAT_family_protein	-3.20
Elen_2526_CDS_ammonium_transporter	-3.48
Elen_0694_CDS_electron_transport_complex,_RnfABCDGE_type,_B_subunit	-3.52
Elen_0695_CDS_electron_transport_complex,_RnfABCDGE_type,_A_subunit	-3.53
Elen_1547_CDS_4Fe-4S_ferredoxin_iron-sulfur_binding_domain_protein	-3.62
Elen_0691_CDS_Heptaprenyl_diphosphate_synthase_component_I	-3.70
Elen_2088_CDS_4Fe-4S_ferredoxin_iron-sulfur_binding_domain_protein	-3.72
Elen_0692_CDS_protein_of_unknown_function_DUF1312	-3.77
Elen_0697_CDS_FMN-binding_domain_protein	-4.07
Elen_0698_CDS_electron_transport_complex,_RnfABCDGE_type,_D_subunit	-4.11
Elen_0693_CDS_ApbE_family_lipoprotein	-4.21
Elen_0696_CDS_electron_transport_complex,_RnfABCDGE_type,_E_subunit	-4.27
Elen_2091_CDS_cysteine_desulfurase,_SufS_subfamily	-4.30
Elen_2090_CDS_hypothetical_protein	-4.96
Elen_1790_CDS_DltD_domain_protein	-5.37
Elen_2089_CDS_Aldehyde_ferredoxin_oxidoreductase	-5.56
Elen_0267_CDS_major_facilitator_superfamily_MFS_1	-5.66
Elen_1420_CDS_capsular_exopolysaccharide_family	-5.94
Elen_0214_CDS_hybrid_cluster_protein	-18.53

*Positive fold-change indicates up-regulation in high arginine.

Table S3.(C) Genes differentially expressed during stationary phase in high versus low arginine (Rank products analysis; % false predictions<0.05, >10-fold change)

Gene identity	Fold-change*
Elen_1880_CDS_NusG_antitermination_factor	73.53
Elen_1186_CDS_major_facilitator_superfamily_MFS_1	29.67
Elen_1190_CDS_molybdopterin_oxidoreductase	22.78
Elen_3011_CDS_SNARE_associated_Golgi_protein	17.04
Elen_2273_CDS_cysteine_desulfurase,_SufS_subfamily	16.84
Elen_1879_CDS_Undecaprenyl-phosphate_galactose_phosphotransferase	16.64
Elen_0107_CDS_flavocytochrome_c	16.37
Elen_3010_CDS_histidine_kinase	15.46
Elen_1806_CDS_riboflavin_biosynthesis_protein_RibF	14.53
Elen_2272_CDS_SufBD_protein	13.95
Elen_0285_CDS_heat_shock_protein_DnaJ_domain_protein	13.77
Elen_3101_CDS_L-carnitine_dehydratase/bile_acid-inducible_protein_F	13.04
Elen_0497_CDS_molydopterin_dinucleotide-binding_region	12.58
Elen_2719_CDS_beta-lactamase_domain_protein	11.99
Elen_1201_CDS_Galactokinase	11.81
Elen_1202_CDS_glycoside_hydrolase_family_2_sugar_binding	10.75
Elen_2133_CDS_translation_elongation_factor_Tu	-10.66
Elen_2679_CDS_Glutathione_peroxidase	-10.77
Elen_2222_CDS_hypothetical_protein	-11.15
Elen_1124_CDS_flavin_reductase_domain_protein_FMN-binding	-11.87
Elen_2528_CDS_hypothetical_protein	-14.16
Elen_0146_CDS_General_substrate_transporter	-14.24
Elen_0297_CDS_hypothetical_protein	-14.51
Elen_0391_CDS_heat_shock_protein_Hsp20	-19.64
Elen_0153_CDS_arginine_deiminase	-22.55
Elen_1568_CDS_C4-dicarboxylate_anaerobic_carrier	-25.19
Elen_0398_CDS_Rubrerythrin	-35.36
Elen_2529_CDS_fumarate_reductase/succinate_dehydrogenase_flavoprotein_domain_protein	-37.55
Elen_0128_CDS_Catalase	-37.98
Elen_0138_CDS_Rubrerythrin	-54.59

*Positive fold-change indicates up-regulation in high arginine.

Table S3.(D) Genes differentially expressed during exponential growth with or without digoxin (Rank products analysis; % false predictions<0.05, >2-fold change)

Gene identity	Fold-change*
Elen_2529_CDS_fumarate_reductase/succinate_dehydrogenase_flavoprotein_domain_protein	175.44
Elen_2528_CDS_hypothetical_protein	156.25
Elen_2125_CDS_conserved_hypothetical_protein	25.71
Elen_0274_CDS_hypothetical_protein	16.50
Elen_0275_CDS_hypothetical_protein	10.15
Elen_0273_CDS_protein_of_unknown_function_DUF322	9.47
Elen_3049_CDS_hypothetical_protein	9.34
Elen_3051_CDS_molybdopterin_oxidoreductase	8.62
Elen_3050_CDS_4Fe-4S_ferredoxin_iron-sulfur_binding_domain_protein	8.33
Elen_3048_CDS_membrane_protein-like_protein	7.75
Elen_0670_CDS_ornithine_carbamoyltransferase	5.72
Elen_0077_CDS_hypothetical_protein	5.18
Elen_1884_CDS_hypothetical_protein	5.06
Elen_0149_CDS_glutamate_decarboxylase	4.57
Elen_0666_CDS_short-chain_dehydrogenase/reductase_SDR	4.38
Elen_2728_CDS_RNA_polymerase,_sigma-24_subunit,_ECF_subfamily	3.72
Elen_2920_CDS_hypothetical_protein	3.51
Elen_1413_CDS_hypothetical_protein	3.46
Elen_0672_CDS_agmatine_deiminase	3.41
Elen_2922_CDS_Aldehyde_ferredoxin_oxidoreductase	3.26
Elen_0673_CDS_carbamate_kinase	3.20
Elen_2231_CDS_hypothetical_protein	3.20
Elen_2499_CDS_histidine_decarboxylase,_pyruvoyl_type	3.13
Elen_0456_CDS_hypothetical_protein	2.96
Elen_2426_CDS_NAD-dependent_epimerase/dehydratase	2.96
Elen_2919_CDS_molybdopterin_oxidoreductase	2.88
Elen_2801_CDS_hypothetical_protein	2.88
Elen_2921_CDS_4Fe-4S_ferredoxin_iron-sulfur_binding_domain_protein	2.86
Elen_2917_CDS_Polysulphide_reductase_NrfD	2.84
Elen_2729_CDS_hypothetical_protein	2.81
Elen_2427_CDS_Spore_coat_polysaccharide_biosynthesis_protein_predicted_glycosyltransferase-	2.77
Elen_0671_CDS_amino_acid_permease-associated_region	2.77
Elen_2500_CDS_amino_acid_permease-associated_region	2.71
Elen_2959_CDS_hypothetical_protein	2.65
Elen_2802_CDS_hypothetical_protein	2.48
Elen_1941_CDS_degV_family_protein	2.47
Elen_2727_CDS_hypothetical_protein	2.39
Elen_1056_CDS_67_kDa_myosin-cross-reactive_antigen_family_protein	2.39
Elen_2924_CDS_hypothetical_protein	2.25
Elen_0706_CDS_acetate/CoA_ligase	2.15
Elen_1599_CDS_Ku_protein	2.07
Elen_0271_CDS_Coproporphyrinogen_III_oxidase-like_Fe-S_oxidoreductase	-2.11
Elen_0742_CDS_protein_of_unknown_function_DUF214	-2.28
Elen_0327_CDS_ABC_transporter_related	-2.46
Elen_0740_CDS_hypothetical_protein	-2.52
Elen_2309_CDS_ABC_transporter_related	-2.59
Elen_0739_CDS_hypothetical_protein	-2.66
Elen_0451_CDS_Polysulphide_reductase_NrfD	-2.67
Elen_2586_CDS_Nitrite_reductase_(cytochrome;_ammonia-forming)	-2.86
Elen_2699_CDS_transcriptional_regulator,_LuxR_family	-2.89
Elen_0520_CDS_transcriptional_regulator,_LuxR_family	-2.96
Elen_1161_CDS_hypothetical_protein	-3.11
Elen_2351_CDS_hypothetical_protein	-3.14
Elen_1740_CDS_hypothetical_protein	-3.14
Elen_0741_CDS_ABC_transporter_related	-3.15
Elen_1742_CDS_4Fe-4S_ferredoxin_iron-sulfur_binding_domain_protein	-3.15
Elen_0267_CDS_major_facilitator_superfamily_MFS_1	-3.25
Elen_0473_CDS_transcriptional_regulator,_LuxR_family	-3.32
Elen_1738_CDS_4Fe-4S_ferredoxin_iron-sulfur_binding_domain_protein	-3.32
Elen_1739_CDS_molybdopterin_oxidoreductase	-3.46
Elen_3096_CDS_major_facilitator_superfamily_MFS_1	-3.49
Elen_1158_CDS_General_substrate_transporter	-3.49
Elen_1160_CDS_Creatininase	-4.01
Elen_1741_CDS_NapD_family_protein	-4.09
Elen_1159_CDS_BCCT_transporter	-4.81
Elen_1162_CDS_protein_of_unknown_function_DUF6_transmembrane	-5.48

*Positive fold-change indicates up-regulation with digoxin.

Table S3.(E) Genes differentially expressed during exponential growth in low arginine with or without digoxin (Rank products analysis; % false predictions<0.05, >2-fold change)

Gene identity	Fold-change*
Elen_2528_CDS_hypothetical_protein	169.49
Elen_2529_CDS_fumarate_reductase/succinate_dehydrogenase_flavoprotein_domain_protein	138.89
Elen_0274_CDS_hypothetical_protein	12.79
Elen_2125_CDS_conserved_hypothetical_protein	12.63
Elen_0706_CDS_acetate/CoA_ligase	11.45
Elen_0275_CDS_hypothetical_protein	10.41
Elen_3048_CDS_membrane_protein-like_protein	9.99
Elen_3049_CDS_hypothetical_protein	9.52
Elen_3050_CDS_4Fe-4S_ferredoxin_iron-sulfur_binding_domain_protein	8.10
Elen_3051_CDS_molybdopterin_oxidoreductase	8.05
Elen_2426_CDS_NAD-dependent_epimerase/dehydratase	6.45
Elen_0707_CDS_hypothetical_protein	5.71
Elen_0077_CDS_hypothetical_protein	5.31
Elen_0273_CDS_protein_of_unknown_function_DUF322	5.22
Elen_2728_CDS_RNA_polymerase,_sigma-24_subunit,_ECF_subfamily	4.83
Elen_1941_CDS_degV_family_protein	4.15
Elen_2727_CDS_hypothetical_protein	3.89
Elen_1884_CDS_hypothetical_protein	3.83
Elen_2959_CDS_hypothetical_protein	3.73
Elen_1427_CDS_Domain_of_unknown_function_DUF1848	3.61
Elen_0676_CDS_ornithine_carbamoyltransferase	3.41
Elen_2191_CDS_ornithine_carbamoyltransferase	-8.62
Elen_0344_CDS_hypothetical_protein	-9.21

*Positive fold-change indicates up-regulation with digoxin.

Table S3.(F) Genes differentially expressed during exponential growth in high arginine with or without digoxin (Rank products analysis; % false predictions<0.05, >2-fold change)

Gene identity	Fold-change*
Elen_2529_CDS_fumarate_reductase/succinate_dehydrogenase_flavoprotein_domain_protein	285.71
Elen_2528_CDS_hypothetical_protein	138.89
Elen_2125_CDS_conserved_hypothetical_protein	45.05
Elen_0274_CDS_hypothetical_protein	19.49
Elen_0273_CDS_protein_of_unknown_function_DUF322	15.02
Elen_3051_CDS_molybdopterin_oxidoreductase	10.59
Elen_0275_CDS_hypothetical_protein	10.00
Elen_0670_CDS_ornithine_carbamoyltransferase	9.20
Elen_3049_CDS_hypothetical_protein	9.07
Elen_3050_CDS_4Fe-4S_ferredoxin_iron-sulfur_binding_domain_protein	8.98
Elen_0149_CDS_glutamate_decarboxylase	7.75
Elen_1884_CDS_hypothetical_protein	6.68
Elen_0666_CDS_short-chain_dehydrogenase/reductase_SDR	6.15
Elen_3048_CDS_membrane_protein-like_protein	5.98
Elen_0077_CDS_hypothetical_protein	5.11
Elen_3032_CDS_hypothetical_protein	4.04
Elen_2499_CDS_histidine_decarboxylase,_pyruvoyl_type	4.03
Elen_2500_CDS_amino_acid_permease-associated_region	3.36
Elen_0676_CDS_ornithine_carbamoyltransferase	-4.72
Elen_1159_CDS_BCCT_transporter	-4.94
Elen_0741_CDS_ABC_transporter_related	-5.64
Elen_0739_CDS_hypothetical_protein	-5.70
Elen_0742_CDS_protein_of_unknown_function_DUF214	-6.23
Elen_1162_CDS_protein_of_unknown_function_DUF6_transmembrane	-6.58
Elen_0740_CDS_hypothetical_protein	-6.63
Elen_1160_CDS_Creatininase	-7.43
Elen_1739_CDS_molybdopterin_oxidoreductase	-7.47
Elen_1740_CDS_hypothetical_protein	-8.40
Elen_1738_CDS_4Fe-4S_ferredoxin_iron-sulfur_binding_domain_protein	-8.72
Elen_1742_CDS_4Fe-4S_ferredoxin_iron-sulfur_binding_domain_protein	-8.74
Elen_1741_CDS_NapD_family_protein	-12.68

*Positive fold-change indicates up-regulation with digoxin.

Table S3.(G) Genes differentially expressed during stationary phase with or without digoxin (Rank products analysis; % false predictions<0.05, >2-fold change)

Gene identity	Fold-change*
Elen_2529_CDS_fumarate_reductase/succinate_dehydrogenase_flavoprotein_domain_protein	62.89
Elen_2528_CDS_hypothetical_protein	37.17
Elen_2921_CDS_4Fe-4S_ferredoxin_iron-sulfur_binding_domain_protein	3.68
Elen_1739_CDS_molybdopterin_oxidoreductase	-4.25
Elen_1186_CDS_major_facilitator_superfamily_MFS_1	-4.36
Elen_1880_CDS_NusG_antitermination_factor	-6.07
Elen_3011_CDS_SNARE_associated_Golgi_protein	-6.93
Elen_3010_CDS_histidine_kinase	-8.03

*Positive fold-change indicates up-regulation with digoxin.

Table S3.(H) Genes up-regulated in stationary phase, low arginine, plus digoxin (Rank products analysis; % false predictions<0.05, >2-fold change)

Gene identity	Fold-change*
Elen_2529_CDS_fumarate_reductase/succinate_dehydrogenase_flavoprotein_domain_protein	158.73
Elen_2528_CDS_hypothetical_protein	112.36
Elen_0465_CDS_cytoplasmic_chaperone_TorD_family_protein	6.85
Elen_2527_CDS_GCN5-related_N-acetyltransferase	6.40

Table S3.(I) Genes down-regulated in stationary phase, high arginine, plus digoxin (Rank products analysis; % false predictions<0.05, >2-fold change)

Gene identity	Fold-change*
Elen_0561_CDS_hypothetical_protein	-2.98
Elen_2721_CDS_single-stranded-DNA-specific_exonuclease_RecJ	-3.27
Elen_1184_CDS_PIN_domain_protein,_putative	-3.39
Elen_2269_CDS_transcriptional_regulator,_BadM/Rrf2_family	-3.65
Elen_1185_CDS_DEAD/DEAH_box_helicase_domain_protein	-3.87
Elen_2820_CDS_chaperonin_GroEL	-3.89
Elen_2335_CDS_hypothetical_protein	-3.93
Elen_2220_CDS_small_GTP-binding_protein	-4.20
Elen_1880_CDS_NusG_antitermination_factor	-4.29
Elen_1088_CDS_transcription_termination_factor_Rho	-4.39
Elen_2066_CDS_putative_transcriptional_regulator,_AsnC_family	-4.51
Elen_2874_CDS_putative_sigma54_specific_transcriptional_regulator	-4.82
Elen_2071_CDS_glutamyl-tRNA_reductase	-5.06
Elen_2842_CDS_two_component_transcriptional_regulator,_winged_helix_family	-5.16
Elen_1810_CDS_translation_initiation_factor_IF-2	-5.20
Elen_0742_CDS_protein_of_unknown_function_DUF214	-5.21
Elen_1949_CDS_arginine_deiminase	-5.24
Elen_3012_CDS_UV-endonuclease_UvdE	-5.45
Elen_2458_CDS_ABC-1_domain_protein	-6.03
Elen_1947_CDS_carbamate_kinase	-6.03
Elen_2333_CDS_aconitate_hydratase_1	-6.12
Elen_2072_CDS_siroheme_synthase	-6.21
Elen_0104_CDS_cell_wall/surface_repeat_protein	-6.60
Elen_1439_CDS_ABC_transporter,_CydDC_cysteine_exporter_(CydDC-E)_family	-6.66
Elen_3010_CDS_histidine_kinase	-6.68
Elen_2285_CDS_pyrroline-5-carboxylate_reductase	-6.91
Elen_2796_CDS_fumarate_reductase/succinate_dehydrogenase_flavoprotein_domain_protein	-7.37
Elen_2585_CDS_hypothetical_protein	-8.29
Elen_1948_CDS_ornithine_carbamoyltransferase	-9.03
Elen_2070_CDS_porphobilinogen_deaminase	-9.22
Elen_2720_CDS_(p)ppGpp_synthetase_I,_SpoT/RelA	-10.67
Elen_2583_CDS_cytochrome_c_assembly_protein	-12.23
Elen_2068_CDS_Radical_SAM_domain_protein	-12.37
Elen_3068_CDS_ATP-dependent_chaperone_ClpB	-12.47
Elen_2286_CDS_cysteine_synthase_A	-14.30
Elen_1946_CDS_C4-dicarboxylate_anaerobic_carrier	-14.79
Elen_2268_CDS_phytoene_desaturase	-15.94
Elen_2069_CDS_uroporphyrin-III_C-methyltransferase	-16.97
Elen_2586_CDS_Nitrite_reductase_(cytochrome;_ammonia-forming)	-46.89

Table S4. *E.lenta* specific primers used for quantitative PCR

Gene	Forward sequence	Reverse sequence	Forward position	Reverse position	Forward melting temp	Reverse melting temp	Product size	Annotation
16S rRNA	CAGCAGGGAAGAAATTCGAC	TTGAGCCCTCGGATTAGAGA	430	588	53.8	55	159	16S rRNA gene
Elen_2528	TGAGGAACCTGTGGTGATCG	CGCCGTGCCTGCTTCCTGCT	6	204	56.7	65.8	199	Cardiac glycoside reductase 1 (*cgr1*)
Elen_2529	TGCGCTGGTCGCAAGGTCTG	CGGCGCGCTTTTTCAGCGTT	425	658	63.0	62.3	234	Cardiac glycoside reductase 2 (*cgr2*)
Elen_2033	TCCTGAGGAGCTGCGAAAGCTG	CGCCCCTAATGCAGTCCCCG	24	141	61.5	63.2	118	LicD family protein
Elen_2416	ACGCACTCGTTCGTACGCGAAA	TCGCATTGCGTTATGAGCCGC	20	147	61.4	60.9	128	Hypothetical protein

Table S5. Clinical usage, and bioavailability information for digoxin, digoxigenin, digitoxin, and ouabain

Compound	Used clinically?	Brand Name	Dosage form	Bioavailability from oral administration	Reference
Digoxin	Yes	Lanoxin	Oral elixir, tablets, injection	60-80%	FDA document; Ref. ID #3195722
Digitoxin	Yes	Crystodigin	Injection, tablets	60-80%	(24)
Digoxigenin	No	-	-	-	-
Ouabain	Yes (Europe)	Strodival	Injection, tablets	43-50%	(25)

Table S6. Genes unique to the *E.lenta* DSM2243 genome (≥1.5 fold-change with digoxin)

Gene	Annotation	BLASTP match	Fold-change (exponential growth, digoxin vs controls)	Genomic loci
Elen_2529*	fumarate reductase/succinate dehydrogenase flavoprotein domain protein	None	174.4	CGR operon
Elen_2528*	hypothetical protein	Non-reciprocal	156.0	CGR operon
Elen_2032	polysaccharide biosynthesis protein	None	1.7	Region1
Elen_2033	LicD family protein	None	1.9	Region1
Elen_2034	glycosyl transferase family 2	None	1.8	Region1
Elen_2415	glycosyl transferase family 2	None	2.4	Region2
Elen_2416	hypothetical protein	None	2.7	Region2
Elen_2417	hypothetical protein	None	1.8	Region2
Elen_2418	glycosyl transferase group 1	None	1.5	Region2
Elen_2419	polysaccharide biosynthesis protein	None	1.5	Region2
Elen_2420	LicD family protein	None	2.2	Region2
Elen_2426*	NAD-dependent epimerase/dehydratase	None	3.0	Region3
Elen_2427*	Spore coat polysaccharide biosynthesis protein predicted glycosyltransferase-like protein	None	2.8	Region3
Elen_2428	protein of unknown function DUF201	None	1.5	Region3
Elen_2959*	hypothetical protein	None	2.6	
Elen_2727*	hypothetical protein	None	2.4	
Elen_2615	protein of unknown function UPF0027	None	2.1	
Elen_2047	hypothetical protein	None	1.9	
Elen_2593	transcriptional regulator, XRE family	None	1.9	
Elen_2726	RNA polymerase, sigma-24 subunit, ECF subfamily	Non-reciprocal	1.8	
Elen_2612	conserved hypothetical protein	None	1.7	
Elen_1635	addiction module antitoxin	None	1.7	
Elen_3059	hypothetical protein	None	1.6	
Elen_0943	hypothetical protein	None	1.6	
Elen_2626	conserved hypothetical protein	None	1.5	
Elen_2027	aminoglycoside phosphotransferase	Non-reciprocal	1.5	
Elen_2532	transcriptional regulator, LuxR family	None	1.5	

*Genes identified as differentially expressed by rank products analysis (Table S3D)

Table S7. Diet information for mouse experiments

Diet name	Manufacturer	Product #	Protein*	Carbohydrate*	Fat*	kcal/g
Standard chow	LabDiet	5021	20.0	53.9	9.0	4.5
0% protein	Harlan Teklad	TD.93328	0.0	81.6	5.5	3.8
20% protein	Harlan Teklad	TD.91352	20.3	61.6	5.5	3.8

* = expressed as % by weight

Table S8. Chow consumption and weight data from mouse experiments

Group	Chow consumed/mouse/day (g)		Weight data (mean±sem g)	
	Standard chow	Custom diet	Fat pad weight	% weight change
Type strain colonization experiment				
0% protein; Type	2.13	2.44	0.64±0.06	-14.9±0.52
20% protein; Type	3.08	2.98	1.35±0.12	0.51±1.54
Type/FAA colonization experiment				
0% protein; Type	4.16±0.08	2.60±0.25	0.39±0.07	-12.1±1.47
20% protein; Type	2.74±0.72	3.58±0.21	0.76±0.04	2.18±1.91
0% protein; 1-3-56	5.00±0.15	2.21±0.15	0.26±0.06	-25.6±2.78
20% protein; 1-3-56	4.89±0.20	3.16±0.10	0.50±0.10	-5.16±2.01

Table S9. Analysis of ileal amino acid content (µg amino acid/mg sample)

	0% protein		*20% protein*		
Amino acid:	**Mean**	**STDEV**	**Mean**	**STDEV**	**Fold change**
ARG	25.3	16.1	37.08	27.04	1.47
HIS	2.88	1.69	4.51	3.19	1.57
LYS	18.47	12.08	25.52	19.72	1.38
TRP	3.88	1.78	6.57	4.64	1.69
LEU	10.87	7.75	21.12	16.53	1.94
PHE	7.17	4.9	13.33	10.44	1.86
VAL	6.44	4.07	11.68	8.88	1.81
MET	3.71	2.43	3.71	2.43	1.00
ALA	16.12	10.88	25.61	19.34	1.59
PRO	2.75	1.62	5.14	4.07	1.87
GLY	5.13	2.91	9.17	6.4	1.79
TYR	8.08	5.27	13.53	10.32	1.67
GLN	6.57	4.06	11.77	9.11	1.79
THR	5.3	3.27	9.74	7.26	1.84
ASN	3.18	1.85	5.97	4.28	1.88
SER	7.78	4.95	14.16	10.55	1.82
GLU	12.14	7.15	22.54	16.25	1.86
ASP	4.38	2.67	8.53	6.25	1.95

Table S10. Multiple reaction monitoring parameters for amino acid analysis

Compound Name	Precursor Ion	Product Ion	Dwell	Fragmentor	Collision Energy	Cell Accelerator Voltage
TRYPTOPHAN	205.1	188.1	50	80	5	4
TYROSINE	182.1	165.1	50	80	5	4
ARGININE	175.1	70.1	50	100	25	4
PHENYLALANINE	166.1	120.1	50	80	9	4
HISTIDINE	156.1	110.1	50	80	13	4
METHIONINE	150.1	56.1	50	70	17	4
GLUTAMATE	148.1	84.1	50	70	13	4
LYSINE	147.1	84.1	50	80	17	4
GLUTAMINE	147.1	84.1	50	70	17	4
ASPARTATE	134	74.1	50	70	13	4
ASPARAGINE	133.1	74.1	50	70	13	4
LEUCINE/ISOLEUCINE	132.1	86.1	50	70	9	4
CYSTEINE	122	59	50	60	25	4
THREONINE	120.1	74.1	50	70	9	4
VALINE	118.1	72.1	50	70	9	4
PROLINE	116.1	70.1	50	80	13	4
SERINE	106.1	60.1	50	70	9	4
ALANINE	90.1	44.1	50	30	9	4
GLYCINE	76	30.1	50	30	9	4

References and Notes:

1. H. J. Haiser, P. J. Turnbaugh, Is it time for a metagenomic basis of therapeutics? *Science* **336**, 1253-1255 (2012).
2. B. D. Wallace *et al.*, Alleviating cancer drug toxicity by inhibiting a bacterial enzyme. *Science* **330**, 831-835 (2010).
3. L. S. Goodman *et al.*, *Goodman & Gilman's the pharmacological basis of therapeutics*. (McGraw-Hill, New York, ed. 12th, 2011).
4. J. Lindenbaum *et al.*, Inactivation of digoxin by the gut flora: reversal by antibiotic therapy. *N. Engl. J. Med.* **305**, 789-794 (1981).
5. C. D. Farr *et al.*, Three-dimensional quantitative structure-activity relationship study of the inhibition of Na(+),K(+)-ATPase by cardiotonic steroids using comparative molecular field analysis. *Biochemistry* **41**, 1137-1148 (2002).
6. J. F. Dobkin *et al.*, Digoxin-inactivating bacteria: identification in human gut flora. *Science* **220**, 325-327 (1983).
7. Materials and methods are available as supplementary materials on *Science* Online.
8. J. F. Sperry, T. D. Wilkins, Arginine, a growth-limiting factor for *Eubacterium lentum*. *J. Bacteriol.* **127**, 780-784 (1976).
9. E. Saunders *et al.*, Complete genome sequence of *Eggerthella lenta* type strain (IPP VPI 0255). *Stand. Genomic Sci.* **1**, 174-182 (2009).
10. K. E. Nelson *et al.*, A catalog of reference genomes from the human microbiome. *Science* **328**, 994-999 (2010).
11. V. I. Mathan, J. Wiederman, J. F. Dobkin, J. Lindenbaum, Geographic differences in digoxin inactivation, a metabolic activity of the human anaerobic gut flora. *Gut* **30**, 971-977 (1989).
12. X. Maymo-Gatell, Y. Chien, J. M. Gossett, S. H. Zinder, Isolation of a bacterium that reductively dechlorinates tetrachloroethene to ethene. *Science* **276**, 1568-1571 (1997).
13. C. F. Maurice, H. J. Haiser, P. J. Turnbaugh, Xenobiotics shape the physiology and gene expression of the active human gut microbiome. *Cell* **152**, 39-50 (2013).
14. Z. Ning, A. J. Cox, J. C. Mullikin, SSAHA: a fast search method for large DNA databases. *Genome Res.* **11**, 1725-1729 (2001).
15. R. Breitling, P. Armengaud, A. Amtmann, P. Herzyk, Rank products: a simple, yet powerful, new method to detect differentially regulated genes in replicated microarray experiments. *FEBS Lett.* **573**, 83-92 (2004).
16. A. Untergasser *et al.*, Primer3--new capabilities and interfaces. *Nucleic Acids Res.* **40**, e115 (2012).

17. S. Kurtz *et al.*, Versatile and open software for comparing large genomes. *Genome Biol.* **5**, R12 (2004).

18. B. Thiele *et al.*, Analysis of amino acids without derivatization in barley extracts by LC-MS-MS. *Anal. Bioanal. Chem.* **391**, 2663-2672 (2008).

19. T. B. Okarma, P. Tramell, S. M. Kalman, The surface interaction between digoxin and cultured heart cells. *J. Pharm. Exp. Ther.* **183**, 559-576 (1972).

20. L. P. Gabel, I. Bihler, P. E. Dresel, Induction of failure in gas-perfused hearts by intermittent administration of Krebs solution. The effect of digitalis glycosides. *Circ. Res.* **21**, 263-269 (1967).

21. W. A. Jacobs, A. Hoffmann, The relationship between the structure and the biological action of the cardiac glucosides. *J. Biol. Chem.* **74**, 482-486 (1927).

22. B. T. Brown, S. E. Wright, Hydrogenation of Digitalis Genins and Anhydrogenins. *J. Pharm. Pharmacol.* **13**, 262-267 (1961).

23. H. M. A. M. Qazzaz, M. A. El-Masri, R. Valdes, Secretion of a lactone-hydrogenated ouabain-like effector of sodium, potassium-adenosine triphosphatase activity by adrenal cells. *Endocrinology* **141**, 3200-3209 (2000).

24. G. G. Belz, K. Breithaupt-Grogler, U. Osowski, Treatment of congestive heart failure--current status of use of digitoxin. *Eur. J. Clin. Invest.* **31 Suppl 2**, 10-17 (2001).

25. H. Furstenwerth, Ouabain - the insulin of the heart. *Int. J. Clin. Pract.* **64**, 1591-1594 (2010).